Article

Cell Reports

Perivascular Mast Cells Govern Shear Stress-Induced Arteriogenesis by Orchestrating Leukocyte Function

Graphical Abstract

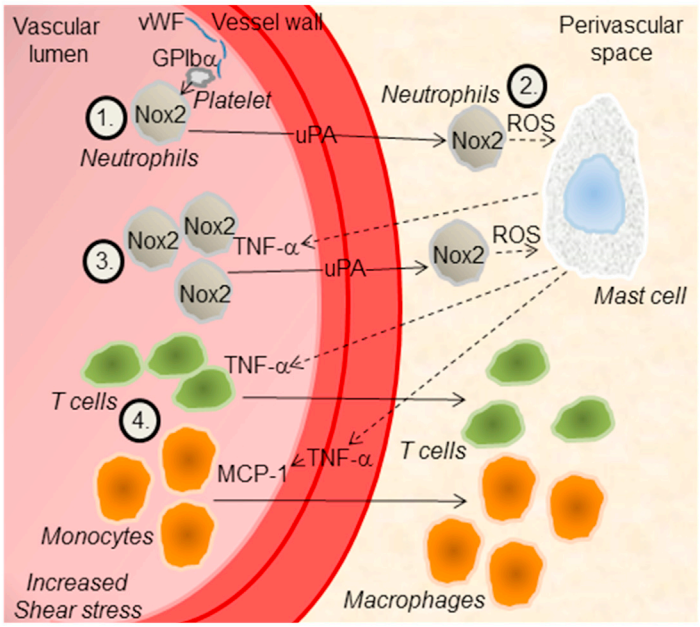

Highlights

- Arteriogenesis is mediated by coordinated action of innate immune cells
- Mast cells orchestrate leukocyte function in arteriogenesis
- Platelet GPIbα is decisive for shear stress-provoked mast cell activation
- Shear stress-induced mast cell activation is mediated by neutrophil-derived ROS

Authors

Omary Chillo, Eike Christian Kleinert, Thomas Lautz, ..., Hanna Mannell, Klaus T. Preissner, Elisabeth Deindl

Correspondence

elisabeth.deindl@med.uni-muenchen.de

In Brief

Increased fluid shear stress is the triggering force for the growth of natural bypasses. How this mechanical load is translated into collateral artery growth is an enigma. Chillo et al. find that mast cell activation governs arteriogenesis by orchestrating leukocyte function.

Chillo et al., 2016, Cell Reports *16*, 2197–2207
August 23, 2016
http://dx.doi.org/10.1016/j.celrep.2016.07.040

Cell Reports
Article

Perivascular Mast Cells Govern Shear Stress-Induced Arteriogenesis by Orchestrating Leukocyte Function

Omary Chillo,[1] Eike Christian Kleinert,[1] Thomas Lautz,[1] Manuel Lasch,[1] Judith-Irina Pagel,[1,2] Yvonn Heun,[1] Kerstin Troidl,[3] Silvia Fischer,[4] Amelia Caballero-Martinez,[1] Annika Mauer,[1,4] Angela R.M. Kurz,[1] Gerald Assmann,[5] Markus Rehberg,[6] Sandip M. Kanse,[7] Bernhard Nieswandt,[8] Barbara Walzog,[1] Christoph A. Reichel,[1,9] Hanna Mannell,[1] Klaus T. Preissner,[4] and Elisabeth Deindl[1,10,*]

[1]Walter-Brendel-Centre of Experimental Medicine, Ludwig-Maximilians-Universität (LMU) Munich, 81377 Munich, Germany
[2]Hospital of the University of Munich, Department of Anesthesiology, LMU Munich, 81377 Munich, Germany
[3]Division of Arteriogenesis Research, Max Planck Institute for Heart and Lung Research, 61231 Bad Nauheim, Germany
[4]Institute for Biochemistry, Medical School, Justus-Liebig-Universität, 35392 Giessen, Germany
[5]Institute of Pathology, LMU Munich, 81377 Munich, Germany
[6]Institute for Stroke and Dementia Research, LMU Munich, 81377 Munich, Germany
[7]Institute of Basic Medical Sciences, University of Oslo, 0372 Oslo, Norway
[8]Institute of Experimental Biomedicine, University Hospital and Rudolf Virchow Center, University of Würzburg, 97080 Würzburg, Germany
[9]Hospital of the University of Munich, Department of Otorhinolaryngology, Head and Neck Surgery, LMU Munich, 81377 Munich, Germany
[10]Lead Contact
*Correspondence: elisabeth.deindl@med.uni-muenchen.de
http://dx.doi.org/10.1016/j.celrep.2016.07.040

SUMMARY

The body has the capacity to compensate for an occluded artery by creating a natural bypass upon increased fluid shear stress. How this mechanical force is translated into collateral artery growth (arteriogenesis) is unresolved. We show that extravasation of neutrophils mediated by the platelet receptor GPIbα and uPA results in Nox2-derived reactive oxygen radicals, which activate perivascular mast cells. These c-kit$^+$/CXCR-4$^+$ cells stimulate arteriogenesis by recruiting additional neutrophils as well as growth-promoting monocytes and T cells. Additionally, mast cells may directly contribute to vascular remodeling and vascular cell proliferation through increased MMP activity and by supplying growth-promoting factors. Boosting mast cell recruitment and activation effectively promotes arteriogenesis, thereby protecting tissue from severe ischemic damage. We thus find that perivascular mast cells are central regulators of shear stress-induced arteriogenesis by orchestrating leukocyte function and growth factor/cytokine release, thus providing a therapeutic target for treatment of vascular occlusive diseases.

INTRODUCTION

Arteries transport oxygenated blood from the heart to every individual organ of the body. Accordingly, occlusion of a major artery by thrombus formation or stenosis results in substantially reduced perfusion of distal organs, leading to ischemic damage or even necrosis of the affected tissue. Current options to treat vascular occlusive diseases such as myocardial infarction, stroke, or peripheral artery disease are percutaneous transluminal angioplasty (PTA) or bypass surgery. However, the body can create natural bypasses from pre-existing arteriolar anastomoses. This so-called arteriogenesis constitutes a tissue and even life-saving process, as it can compensate for the loss of a major peripheral or coronary artery. Promoting arteriogenesis in ischemia-related diseases may present a non-invasive alternative therapeutic approach to established clinical interventions.

Arteriogenesis is a complex, multi-factorial process (Deindl and Schaper, 2005) that involves the proliferation of endothelial cells (ECs) and smooth muscle cells (SMCs) as well as the recruitment of leukocytes, especially monocytes, which provide a variety of growth-promoting factors to the growing blood vessel (Arras et al., 1998). It is, therefore, not surprising that the therapeutic use of single growth factors or cytokines to support arteriogenesis did not meet expectations in clinical studies. To effectively promote arteriogenesis in patients, it is important to identify the molecular mechanisms naturally triggering the process of collateral artery growth.

Mast cells reside in the perivascular space of arteries (Wolf et al., 1998) and produce several vasoactive substances and growth factors (Hiromatsu and Toda, 2003; Rao and Brown, 2008), some of which have been described to contribute to arterial remodeling (Cao et al., 2003; Ito et al., 1997). The functional role of these c-kit$^+$/CXCR4$^+$ cells in arteriogenesis is currently unclear. Moreover, how fluid shear stress, which is the driving force for arteriogenesis (Pipp et al., 2004) and is sensed directly by vascular ECs, is translated into the activation of perivascular mast cells remains unresolved. Here we dissect the underlying

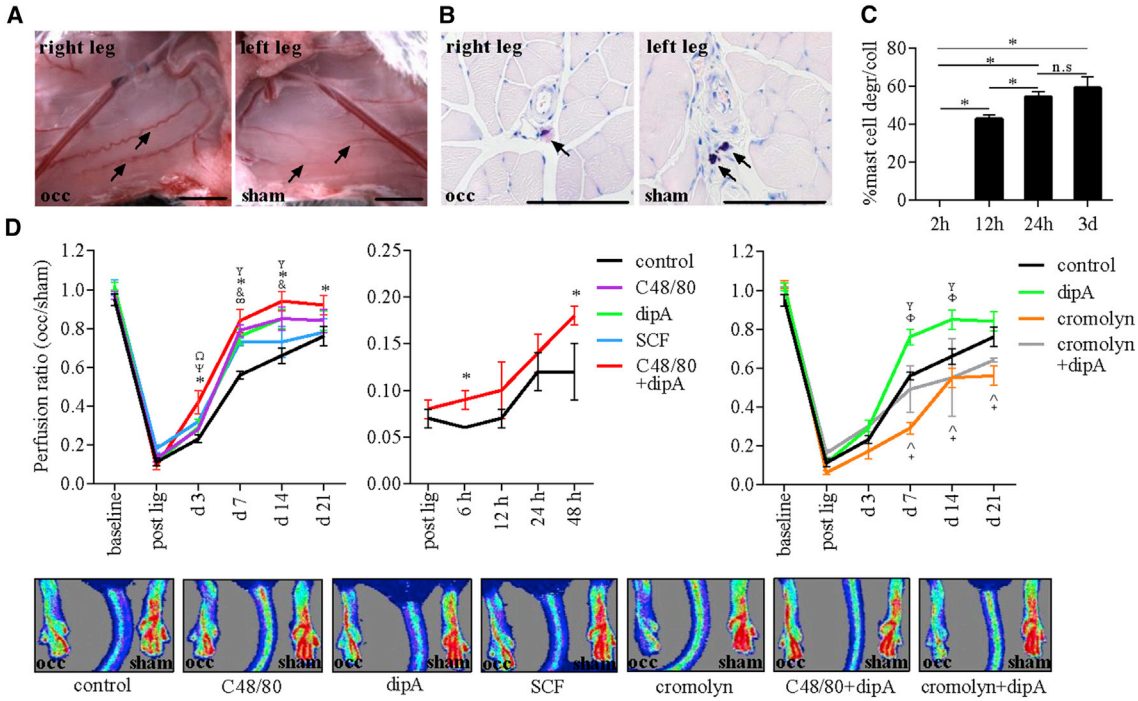

Figure 1. Collateral Artery Growth Is Fostered by Activated Mast Cells

(A) Photographs of superficial collateral arteries (arrows) in the medial adductor hindlimb region of a mouse. Right: pre-existing collaterals on the left sham-operated leg are observed as thin vessels running in a straight line. Left: grown collateral arteries of the occluded right leg (occ) have drastically increased in diameter and appear in a typical corkscrew formation. Pictures were taken 21 days after the surgical procedure. Scale bar, 1 mm; n = 3.

(B) Representative Giemsa staining reveals mast cell degranulation next to growing collaterals (arrow left), whereas sham operation had no effect on mast cells (arrows right). Pictures were taken 3 days after the surgical procedure. Scale bar, 100 μm; n = 6.

(C) Mast cell degranulation is shown per collateral 2 hr, 12 hr, 24 hr, and 3 days after fal (n = 4 animals with four collaterals/time point; *p ≤ 0.05 from two-way ANOVA with Newman-Keuls test).

(D) Laser Doppler perfusion measurements of wild-type mice following fal (right leg) and sham operation (left leg). Upper panels: perfusion was calculated by means of laser Doppler right-to-left ratios before, immediately after, and at 6, 12, 24, and 48 hr (middle panel) or at days 3, 7, 14, and 21 after the surgical procedure (right and left panels). Color-coded lines indicate treatment of mice (control = saline). Control and internal control (dipA) of the right plot are identical to that of the left plot. Statistical analysis (p ≤ 0.05) was performed between different groups (n = 6 per group) using repeated-measures two-way ANOVA with subsequent multiple comparisons by Bonferroni test ($^{\&}$C48/80 versus control; ^{Y}dipA versus control; $^{\infty}$SCF versus control; *C48/80 + dipA versus control; $^{\Omega}$C48/80 + dipA versus dipA; $^{\Psi}$C48/80 + dipA versus C48/80; $^{\Lambda}$cromolyn versus control; $^{+}$cromolyn versus dipA; and $^{\Phi}$cromolyn + dipA versus dipA). Lower panels: representative flow images of day 7 are shown.

Data are means ± SEM. See also Figure S1.

mechanisms, finding a decisive role for platelets and neutrophils in this process. In particular we find that platelet receptor GPIbα-dependent and urokinase plasminogen activator (uPA)-mediated extravasation of neutrophils culminates in mast cell activation by reactive oxygen species (ROS) produced by neutrophil-expressed Nox2. Furthermore, following natural or pharmacological activation, we find that mast cells promote arteriogenesis by creating an inflammatory microenvironment essential for the recruitment of growth-promoting leukocytes. Thus, mast cells might represent a therapeutic target for the treatment of vascular occlusive diseases.

RESULTS

Mast Cell Activation Fosters Experimental Arteriogenesis

To study the functional impact of mast cells in arteriogenesis, we used an experimental murine hindlimb model in which femoral artery ligation (fal) resulted in collateral artery growth in the upper leg (Figure 1A) (Limbourg et al., 2009). Our results showed that, upon fal, mast cells located in the perivascular space of collaterals became activated and gradually but specifically degranulated (Figures 1B and 1C). Moreover, treatment of mice with the mast cell activator Compound 48/80 (C48/80); the c-kit ligand stem cell factor (SCF), which triggers mast cell maturation and recruitment (Oliveira and Lukacs, 2003); or diprotin A (dipA) (for protocols, see Figure 7 and Supplemental Experimental Procedures), respectively, significantly enhanced perfusion recovery upon fal (Figure 1D). DipA treatment, inhibiting dipeptidylpeptidase IV (DPPIV) activity and, thereby, retarding stroma cell-derived factor-1 (SDF-1α) degradation (Zaruba et al., 2009), resulted in an increased level of SDF-1α (Figure S1A) and drastically increased the number of c-kit^{+} cells (Figure S1B). In accordance with previous findings (McGowen et al., 2009), C48/80 treatment provoked enhanced mast cell degranulation, culminating in a

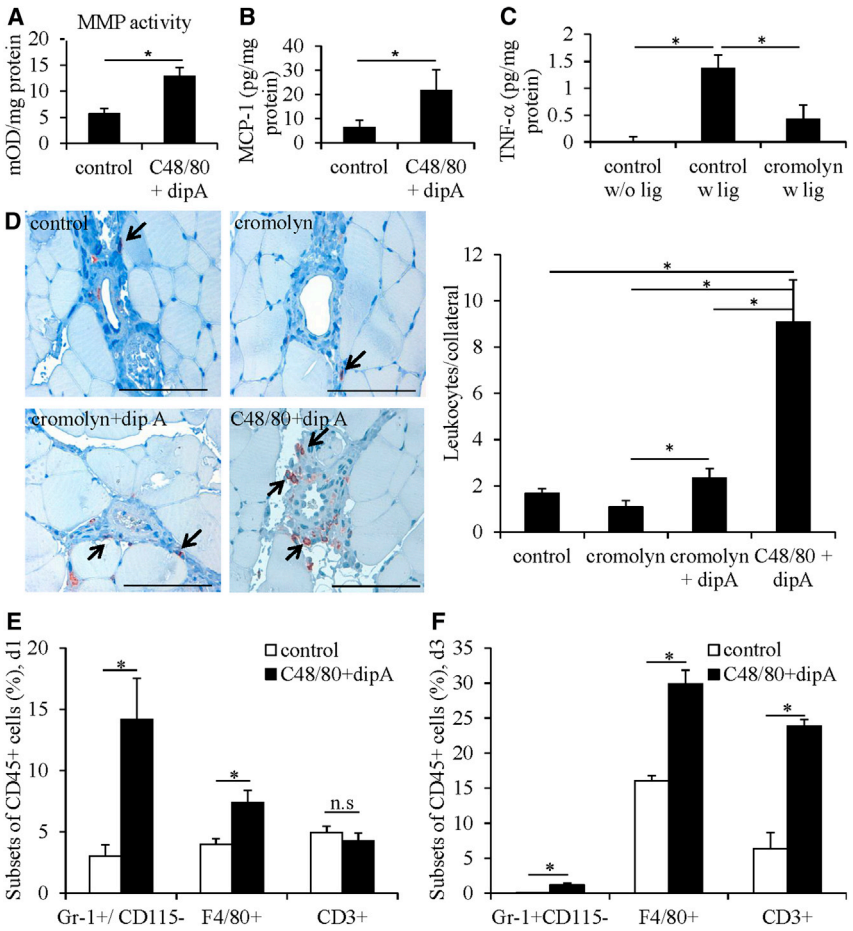

Figure 2. C48/80 + DipA Treatment Fosters Leukocyte Recruitment

(A) Proteolytic activity of matrix metalloproteinases (MMPs) was measured in collaterals of mice 24 hr after fal and saline (control) or C48/80 + dipA treatment (n = 3).

(B) MCP-1 protein levels were measured in collaterals of mice treated with saline (control) or C48/80 + dipA 24 hr after fal (n = 3).

(C) TNF-α levels were measured in plasma of mice without fal (control w/o lig) or 24 hr after fal and saline (control w lig) or cromolyn treatment (cromolyn w lig) (n = 3 per group).

(D) Left: representative immunostaining showing CD45-positive cells (arrows) in the perivascular region of collaterals of saline- (control), cromolyn-, cromolyn + dipA-, and C48/80 + dipA-treated animals 3 days after fal. Right: quantitative analysis is shown. Scale bars, 100 μm; n = 4 animals with four collaterals each.

(E and F) Quantitative analyses by flow cytometry of $CD45^+/CD11b^+/Gr\text{-}1^+/CD115^-$, $CD45^+/CD11b^+/F4/80^+$, and $CD45^+/CD3^+$ cells in adductor muscles of mice at day 1 (E) and day 3 (F) after fal and saline (control, open bars) or C48/80 + dipA (filled bars) treatment (n = 6 per group; *p ≤ 0.05 in (C) and (D) from two-way ANOVA with Newman-Keuls test).

Data are means ± SEM. See also Figures S2 and S3.

drastic reduction in the numbers of detectable mast cells in the vicinity of collateral arteries (93% ± 4.6% reduction, $p < 0.05$). Combined administration of C48/80 and dipA further increased perfusion recovery, reaching significant values already 6 hr after fal (Figure 1D), whereas combined treatment of mice with C48/80, dipA, and SCF showed no further additive effect (Figure S1C).

Simultaneous treatment of mice with dipA and the mast cell stabilizer cromolyn was performed to exclude the possibility that the positive effect of dipA was not mainly due to the mobilization of other bone marrow-derived cells also expressing the SDF-1α receptor CXCR-4 (e.g., monocytes and stem cells). Cromolyn treatment abolished the stimulating effect of dipA and impaired perfusion recovery (Figure 1D) to a similar extent as observed with single cromolyn treatment (Figure 1D), indicating that the majority of recruited cells were indeed mast cells that promoted arteriogenesis by their degranulation products. Cromolyn treatment also blocked the positive effect of C48/80 (Figure S1D).

Mast cell-deficient $Mcpt5\text{-}Cre^+$ R-DTA mice showed no reduced perfusion recovery upon the induction of arteriogenesis. Intriguingly, these mice responded neither to cromolyn nor to C48/80 treatment (Figure S1E). These data indicate that these transgenic mice were capable of compensating the lack of mast cells in arteriogenesis; yet, cromolyn as well as C48/80, specifically influenced the action of mast cells or, if at all, did not influence decisively other cells or off targets relevant for the process of collateral artery growth in wild-type mice.

Combined Treatment of Mice with C48/80 and DipA Promotes Leukocyte Recruitment and Vascular Cell Proliferation

Matrix metalloproteinases (MMPs), which are well described to be activated by mast cell-derived proteases (Kovanen, 2007), degrade and remove basement membrane proteins around SMCs (Rudijanto, 2007) and have been shown to promote vascular remodeling in the context of arteriogenesis (Cai et al., 2000). In growing collaterals of mice treated with C48/80 + dipA, we found significantly increased MMP activity compared to saline-treated controls (Figure 2A).

MCP-1 and tumor necrosis factor α (TNF-α) are two cytokines previously reported to be of major relevance for leukocyte recruitment in the process of arteriogenesis (Grundmann et al., 2005; Ito et al., 1997). Here mice treated with C48/80 + dipA showed significantly increased mRNA and protein levels of MCP-1 compared to saline-treated controls (Figures 2B and S2). In contrast, cromolyn treatment strongly reduced the plasma level of TNF-α as compared to saline-treated controls (Figure 2C), indicating that mast cells play a major role in providing this cytokine being relevant for leukocyte recruitment (Malaviya et al., 1996).

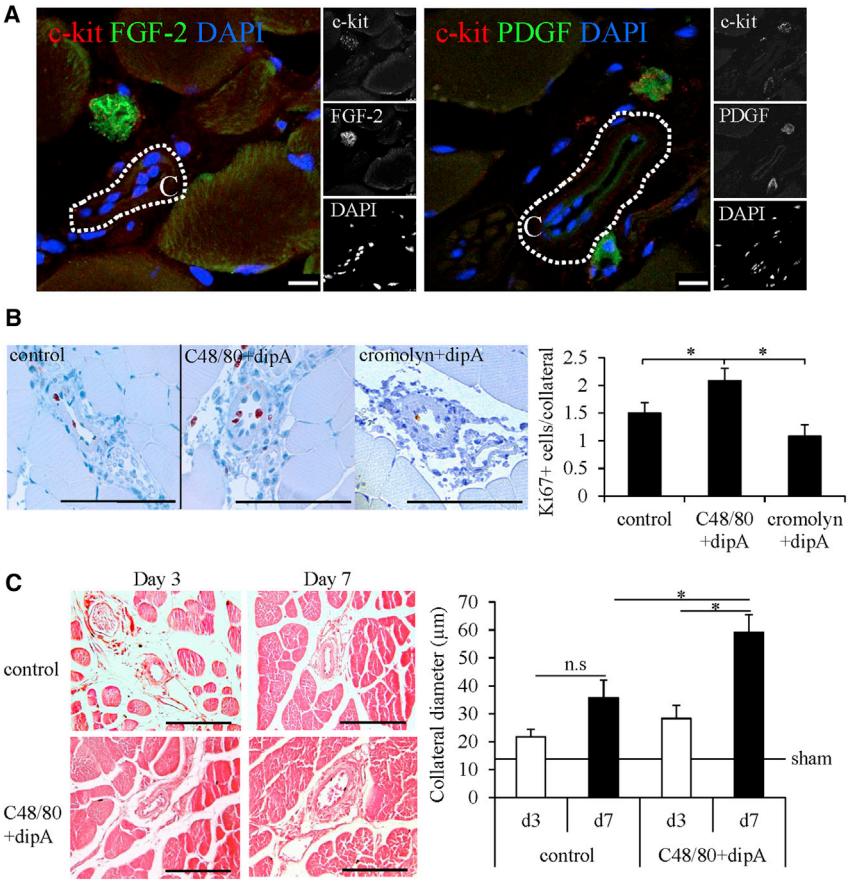

Figure 3. Mast Cells Promote Vascular Cell Proliferation and Vessel Growth

(A) Representative fluorescent immunohistological pictures of collaterals of mice 2 hr after fal. c-kit$^+$ cells in close proximity to collaterals (marked by dotted lines) stain positive for FGF-2 and PDGF-BB. Scale bar, 10 μm; n = 6 slices from three individual experiments.

(B) Left: representative immunostaining showing Ki67$^+$ cells (stained in brown) in collaterals of mice treated with saline (control), C48/80 + dipA, or cromolyn + dipA 3 days after fal. Right: quantitative analysis is shown. Scale bar, 100 μm; n = 3 animals with four collaterals each.

(C) Left: representative HE staining documenting collaterals of mice treated with saline (control) or C48/80 + dipA at day 3 or 7 after fal. Right: chart shows inside luminal diameter of collaterals of mice treated with saline (control) or C48/80 + dipA at day 3 and 7 after fal or sham operation.

Scale bar, 100 μm; n = 3 animals with three collaterals each; *p ≤ 0.05 (B and C) from two-way ANOVA with Newman-Keuls test. Data are means ± SEM. See also Figure S4.

Immunohistological analyses of the adductor muscle revealed significantly increased numbers of CD45$^+$ (pan leukocyte marker) cells in the perivascular space of C48/80 + dipA-treated mice (Figure 2D). Subset analyses of recruited CD45$^+$ cells by flow cytometry showed significantly increased levels of neutrophils (Gr-1$^+$/CD115$^-$) and macrophages (F4/80$^+$) at day 1 after fal (Figures 2E and S3A) and neutrophils, macrophages, and T cells (CD3$^+$) at day 3 after fal (Figures 2F and S3B). The latter represents a subset of leukocytes previously described to invade tissue in a TNF-α-dependent manner (Maggi et al., 2013) and to be involved in arteriogenesis (Stabile et al., 2006). Regarding the recruitment of subsets of CD45$^+$ cells at day 1 and day 3 after fal, a similar although less drastic effect was observed in mice treated with C48/80 alone (Figures S3C and S3D).

Treatment of primary vascular ECs and SMCs with conditioned medium of activated mast cells increased their proliferation rate (Figure S4). Moreover, fibroblast growth factor (FGF)-2 and platelet-derived growth factor (PDGF)-BB was found in mast cells located in close proximity to collateral arteries (Figure 3A). A combined administration of both growth factors previously has been described to enhance arteriogenesis (Cao et al., 2003). Mice treated with combined C48/80 + dipA revealed an increased number of Ki67$^+$ (cell proliferation marker) vascular cells in collateral arteries (Figure 3B), which was associated with an increased luminal diameter of these blood vessels (Figure 3C). In contrast, combined treatment with cromolyn + dipA reduced the number of Ki67$^+$ vascular cells (Figure 3B). Altogether these data suggest that mast cells promote vascular cell proliferation, not only indirectly by promoting leukocyte recruitment supplying growth-promoting factors but also by themselves representing a source of vascular growth factors.

Boosting Mast Cell Recruitment and Activation Protects Tissue from Damage by Fostering Arteriogenesis

Upon ligation of the femoral artery in the upper leg, the resulting reduced perfusion of the lower leg was associated with ischemic damage, provoking increased infiltration of leukocytes and capillary sprouting (angiogenesis). Both processes are necessary for removing fibrotic and necrotic tissue. Since our data demonstrate that combined treatment of mice with C48/80 + dipA significantly increased perfusion recovery already 6 hr after fal (Figure 1D), we hypothesized that this is associated with reduced damage of the distal calf muscle (Figure S5). Histological analysis of the gastrocnemius muscle revealed almost negligible ischemic tissue damage in mice treated with C48/80 + dipA (Figure 4A). This was associated with (1) a significantly reduced infiltration of leukocytes (CD45$^+$ cells) (Figure 4B) as well as (2) a diminished capillary sprouting, as shown by the reduced number of Ki67$^+$ ECs (Figure 4C) and a reduced capillary-to-muscle fiber ratio (Figure S6). Interestingly, neither fal nor local application of C48/80 in the upper leg resulted in mast cell degranulation in the ipsilateral lower leg (M. gastrocnemius) (Figure 4D) or in the contralateral upper or lower leg (data not shown). These data indicate that local application of C48/80 in the upper leg did not result in systemic effects of the agent. Additionally, the

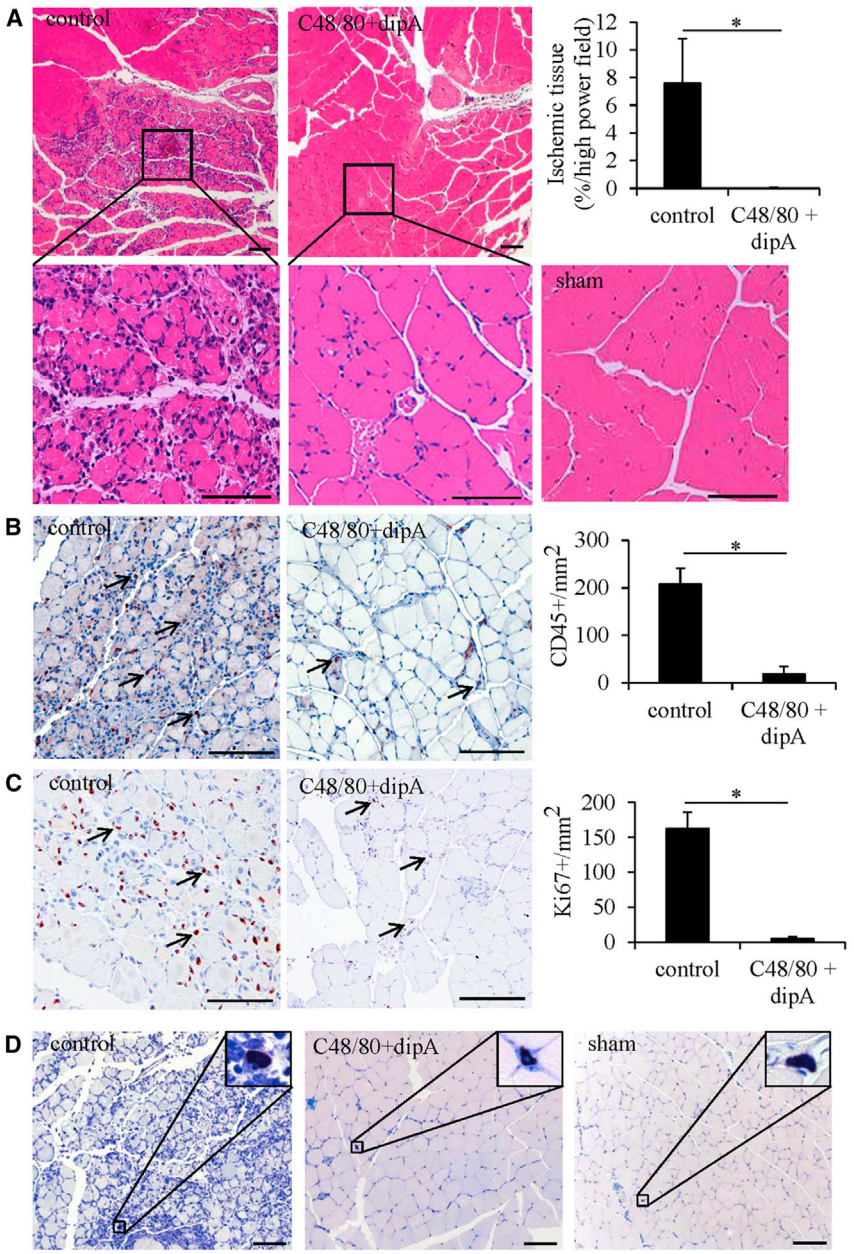

Figure 4. Effective Arteriogenesis Protects Tissue from Severe Ischemic Damage

(A) Representative HE staining of gastrocnemic muscles 3 days after fal (control) or sham operation or 3 days after fal and C48/80 + dipA treatment in different magnifications. Scale bar, 100 μm. Bar graph represents ischemic tissue in the M. gastrocnemius in percentage of high-power field.

(B) Left: representative pictures of immunostaining show reduced infiltration of leukocytes ($CD45^+$ cells, arrows, stained in brown) in the M. gastrocnemius of mice treated with C48/80 + dipA compared to saline- (control) treated mice 3 days after fal. Scale bar, 100 μm. Right: quantitative analysis is shown.

(C) Left: following fal, representative pictures document Ki67-positive capillaries (arrows, stained in brown) in the M. gastrocnemius of saline- (control) or C48/80-treated mice 3 days after fal. Scale bar, 100 μm. Right: number of Ki67-positive capillaries was quantified.

(D) Representative Giemsa staining of the M. gastrocnemius of mice treated with saline (control) or C48/80 + dipA 3 days after fal or sham operation. Insets show magnifications of mast cells.

Scale bar, 100 μm; n = 3 in triplicates (A–D). Data are means ± SEM. See also Figures S5 and S6.

data suggest that protection of tissue from ischemic damage was a result of arteriogenesis in the upper leg, but not due to degranulation of mast cells in the lower leg.

Perivascular Mast Cells Are Activated by a Cascade of Platelet- and Neutrophil-Dependent Reactions

Fluid shear stress, which is the driving force behind arteriogenesis, can only be sensed directly by vascular ECs, but not by perivascular cells. Hence, we asked which factors or cells may be responsible for mast cell degranulation during the initial phase of arteriogenesis. As platelets are sensors of fluid shear stress and can adhere to endothelial von Willebrand factor (vWF) under conditions of increased fluid shear stress through platelet GPIb receptor (Sadler, 2002), we hypothesized that platelets or platelet-dependent reactions may be involved in transmitting molecular signals from the vascular lumen to the perivascular space.

Interestingly, blockage of the platelet receptor GPIbα as well as genetic ablation of the ectodomain of GPIbα in transgenic IL4-R/Iba mice inhibited mast cell degranulation to a similar extent as cromolyn treatment (Figure 5A). Similarly, uPA deficiency or the inhibition of uPA proteolytic activity by the administration of UK122 significantly diminished mast cell degranulation (Figure 5A).

We have shown previously that uPA deficiency (but not uPA receptor or tissue plasminogen activator deficiency) is associated with a reduced perfusion recovery upon fal, which was due to reduced leukocyte infiltration (day 3 after fal) (Deindl et al., 2003). Recently, we observed a reduced reperfusion recovery upon fal when blocking the GPIbα receptor using a Fab fragment. Furthermore, the same effect was seen in GPIbα receptor-deficient IL4-R/Iba mice. Of note, our results evidenced that the GPIbα receptor is essential in arteriogenesis for (1) transient platelet interaction with collateral endothelium, (2) differential expression of vascular uPA (day 1 after fal), (3) platelet-neutrophil aggregate (PNA) formation (day 1 after fal), and (4) extravasation of leukocytes (3 days after fal) (Chandraratne et al., 2015). Furthermore, in a model of hepatic ischemia reperfusion injury, we found endothelial-derived uPA to be essential for intravascular adherence of neutrophils. Moreover,

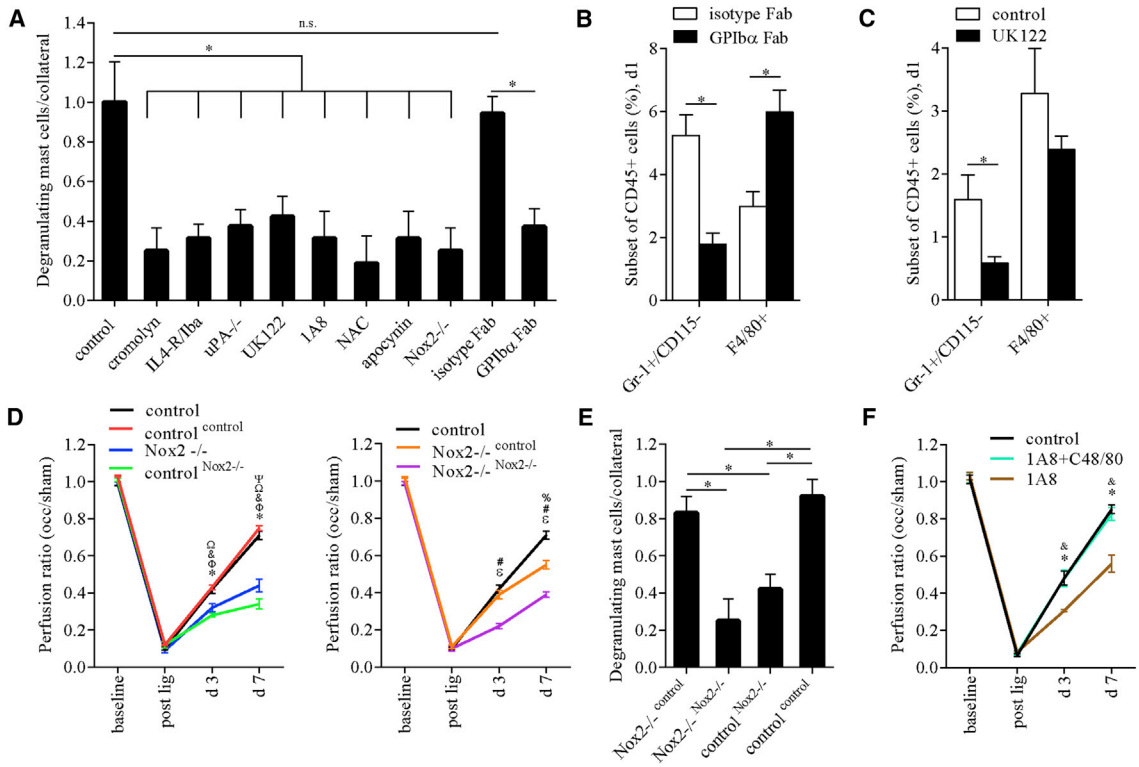

Figure 5. Mast Cells Are Activated by Neutrophil-Derived ROS

(A) Degranulated mast cells in the perivascular space of collaterals 1 day after fal in control mice or in mice treated with cromolyn to stabilize mast cells; UK122 (uPA inhibition); 1A8 (neutrophil-depleting agent); N-actelcysteine (NAC, ROS scavenger); apocynin (NADPH oxidase inhibitor); GPIbα-blocking Fab fragment; isotype Fab fragment; and in mice deficient for platelet receptor GPIbα (IL4-R/Iba mice), uPA, or Nox2, respectively, are shown (n = 4 animals with two collaterals each).

(B and C) Flow cytometry analysis of $CD45^+/CD11b^+/Gr\text{-}1^+/CD115^-$ and $CD45^+/CD11b^+/F4/80^+$ cells in adductor muscles of animals treated with GPIbα-blocking Fab fragment or isotype Fab fragment (B) or uPA inhibitor UK122 or control group (C) at day 1 after fal is shown (n = 4).

(D) Laser Doppler perfusion measurements of (left panel) wild-type mice (control), Nox2-deficient mice (Nox2−/−), wild-type mice reconstituted with bone marrow from wild-type mice ($control^{control}$), and wild-type mice reconstituted with bone marrow from Nox2-deficient mice ($control^{Nox2-/-}$) and (right panel) wild-type mice (control), Nox2-deficient mice reconstituted with bone marrow from Nox2-deficient mice ($Nox2-/-^{Nox2-/-}$), and Nox2-deficient mice reconstituted with bone marrow from wild-type mice ($Nox2-/-^{control}$) after the induction of arteriogenesis (right leg) or sham operation (left leg) at the indicated time points after the surgical procedure. Color-coded lines indicate different groups. The controls of the left and right plot are identical. Statistical analysis ($p \leq 0.05$) was as follows: *Nox2−/− versus control; $^{\Phi}control^{Nox2-/-}$ versus control; $^{\&}Nox2-/-$ versus $control^{control}$; $^{\Omega}control^{Nox2-/-}$ versus $control^{control}$; $^{\psi}control^{Nox2-/-}$ versus Nox2−/−; $^{\#}Nox2-/-^{Nox2-/-}$ versus control; $^{\epsilon}Nox2-/-^{Nox2-/-}$ versus $Nox2-/-^{control}$; and $^{\%}Nox2-/-^{control}$ versus control (n = 5 per group).

(E) Degranulated mast cells in the perivascular space of growing collaterals 1 day after fal in $Nox2-/-^{control}$, $Nox2-/-^{Nox2-/-}$, $control^{Nox2-/-}$, and $control^{control}$ mice are shown (n = 6 slices from three individual animals with two collaterals each).

(F) Laser Doppler perfusion measurements of saline- (control), 1A8-, or 1A8 + C48/80-treated wild-type mice following fal (right leg) and sham operation (left leg) (n = 6 per group). Statistical analysis ($p \leq 0.05$) was as follows: $^{\&}$control versus 1A8 and *1A8+C48/80 versus 1A8.

Data are means ± SEM. Significances (*$p \leq 0.05$) in (A) and (E) were from two-way ANOVA with Newman-Keuls test, and significances in (D) and (F) were from repeated-measures two-way ANOVA with subsequent multiple comparisons by Bonferroni test. See also Figure S7.

neutrophil-derived uPA was critical for subsequent paracellular transmigration of neutrophils and, hence, extravasation (Reichel et al., 2011). We therefore hypothesized that neutrophils also may play a role in arteriogenesis and may represent the missing link in mast cell activation. Indeed, inhibition of GPIbα receptor or uPA activity resulted not only in reduced mast cell activation but also in diminished neutrophil infiltration at day 1 after fal, as assessed by flow cytometry (Figures 5B and 5C).

To analyze the functional relevance of neutrophils and PNA formation in more detail, we performed in vitro studies using isolated platelets and neutrophils. We found that PNA formation is a prerequisite for surface expression of uPA on neutrophils as well as for extracellular superoxide anion formation (Figures S7A–S7D). P-selectin deficiency on platelets as well as deficiency of its ligand PSGL-1 on neutrophils interfered with PNA formation and diminished uPA surface expression (Figures S7A–S7C). In addition, P-selectin deficiency of platelets prevented superoxide anion formation (Figure S7D), accounting for the relevance of platelet P-selectin for the production of neutrophil-derived ROS (Page and Pitchford, 2013). Finally, extracellular ROS production was absent when using Nox2-deficient neutrophils for PNA formation, indicating that neutrophils are the source of superoxide anions (Figure S7D). A proposed model for neutrophil activation during arteriogenesis is shown in Figure S7E.

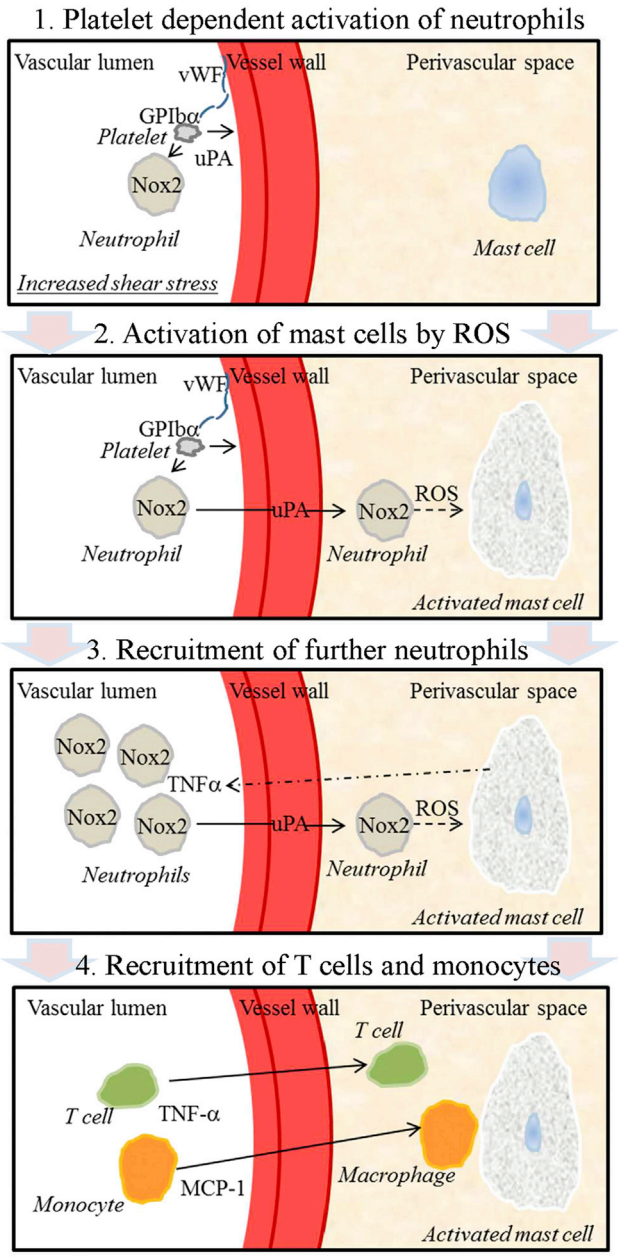

Figure 6. Proposed Model for the Central Role of Mast Cells in Arteriogenesis

Step 1. Upon occlusion of a main artery, increased fluid shear stress in collateral arteries initiates GPIbα-dependent PNA formation, which results in the activation of neutrophils. Step 2. After uPA-mediated extravasation of neutrophils, Nox2-derived superoxide anions (ROS) induce mast cell degranulation. Step 3. TNF-α promotes further neutrophil extravasation in a positive feedback loop. Step 4. TNF-α supports T cell extravasation and MCP-1 attracts monocytes, which mature to macrophages and supply the growing vessel with growth factors and cytokines. See also Figure S7E.

To assess whether Nox2-derived ROS from neutrophils are relevant for mast cell degranulation during arteriogenesis, we performed further in vivo analyses. Indeed, our results showed that depletion of neutrophils by the application of 1A8 (reduction of neutrophils: 70% ± 3.7%, $p < 0.05$), deficiency of Nox2 (= gp91phox), as well as blocking ROS production or their function by the administration of apocynin or N-acetylcysteine (NAC) (Schulz et al., 2014; Tobar et al., 2010), respectively, blocked mast cell degranulation to a similar degree as observed in GPIbα-deficient mice (Figure 5A). To investigate whether neutrophil-derived ROS are responsible for mast cell degranulation, we created chimeric mice by transplanting bone marrow from Nox2−/− mice to wild-type mice (control$^{Nox2-/-}$) and vice versa (Nox2−/−^{control}). Compared to their corresponding control (control^{control}), control$^{Nox2-/-}$ showed a significant reduction in perfusion recovery as well as mast cell degranulation, whereas Nox2−/−^{control} revealed a significant improvement in collateral formation as compared to control (Nox2−/−$^{Nox2-/-}$) (Figures 5D and 5E). To confirm that mast cells become activated by ROS derived from neutrophils, neutropenic mice were challenged with C48/80 to induce mast cell degranulation. While neutrophil depletion impaired perfusion recovery after fal, the induction of mast cell degranulation completely restored the phenotype (Figure 5F).

DISCUSSION

In this study, we show that natural bypass growth is a matter of innate immunity, and we highlight the central role of mast cells in orchestrating leukocyte function in this process. In addition, we deciphered the mechanisms responsible for the translation of increased fluid shear stress to the activation of perivascular mast cells (Figure 6).

Mast cells were found to reside in the perivascular space of growing collaterals (Wolf et al., 1998). However, their function in arteriogenesis has never been investigated. Moreover, the mechanism by which perivascular mast cells become activated by increased mechanical load, such as fluid shear stress, has not been resolved up to now. We demonstrate that this is mediated by platelets and neutrophils and that neutrophil-derived ROS are the driving force for mast cell activation.

Fluid shear stress, which stimulates arteriogenesis, is well described to induce the adherence of platelets to ECs, a process mediated by the interaction of the platelet receptor GPIbα with the endothelial vWF (Sadler, 2002). We recently demonstrated that platelet receptor GPIbα is essential for the transient interaction of platelets to collateral endothelium, PNA formation, and extravasation of leukocytes during arteriogenesis (Chandraratne et al., 2015). Here we show that platelet receptor GPIbα is particularly relevant for neutrophil extravasation. We demonstrate that PNA formation through platelet P-selectin and neutrophil PSGL-1 is associated with uPA release to the neutrophil cell surface, paving the way for leukocyte infiltration. Moreover, we found that PNA formation is a prerequisite for neutrophil Nox2-dependent superoxide anion release.

As the deficiency or inhibition of uPA resulted in diminished neutrophil extravasation and mast cell degranulation, it is fair to deduce that the activation of neutrophils through interaction with platelets not only drives extravasation of these cells via uPA but also promotes mast cell activation via the release of neutrophil superoxide anions. This conclusion is endorsed by

our findings showing (1) a rescue of the impaired reperfusion recovery and mast cell degranulation observed in Nox2−/− mice by the transplantation of bone marrow isolated from wild-type mice, and (2) restored perfusion in neutropenic mice by the induction of mast cell degranulation. These in vivo data are affirmed by in vitro findings showing that ROS stimulate mast cell activation (Gan et al., 2015) as well as by our results showing that activated neutrophils induce mast cell degranulation (Figure S7F). Together, these data indicate that the intravascular, shear stress-dependent activation of platelets and PNA formation triggers the production of effectors, such as ROS, that serve to transmit the locally initiated signal to proximal perivascular sites where mast cell degranulation is initiated.

Interestingly enough, platelet activation, uPA-mediated neutrophil extravasation, as well as mast cell activation recently were shown to contribute to reperfusion injury due to revascularization or organ transplantation (Chang et al., 2014; Egashira et al., 2013; Köhler et al., 2011; Reichel et al., 2011; Yang et al., 2014). In addition, allergic contact dermatitis was reported to strongly depend on mast cells, neutrophils, and neutrophil-derived ROS (Weber et al., 2015). Thus, the mechanisms identified in this study for mast cell activation under arteriogenic conditions appear to have a strong and more general impact, not just on pathogenesis and control of cardiovascular diseases, and they will contribute to the understanding of mast cell-dependent pathways in sterile inflammation/innate immunity.

In our study, we found mast cells to specifically degranulate around growing collateral arteries. Additional pharmacological activation of mast cells with C48/80 greatly enhanced perfusion recovery and, hence, arteriogenesis. Stabilizing mast cells with cromolyn showed the opposite effect and blocked the positive effect of C48/80 as well as dipA. Mast cell-deficient Mcpt5-Cre$^+$ R-DTA mice showed no reduced perfusion recovery upon fal, neither was it improved by C48/80 treatment nor impaired by cromolyn. These data suggest that these transgenic mice were capable of compensating the lack of mast cells in the process of arteriogenesis and that cromolyn as well as C48/80 specifically and decisively influenced the action of mast cells in the process of collateral artery growth in wild-type mice.

TNF-α is a major determinant in neutrophil recruitment, as evidenced in many experimental settings (Griffin et al., 2012; Malaviya et al., 1996). Our results demonstrate that inhibition of mast cell degranulation strongly reduced the elevated plasma levels of TNF-α observed upon the induction of arteriogenesis. C48/80 treatment, in contrast, resulted in an increased number of neutrophils, especially at day 1 after fal (Figure S3C). These data indicate that neutrophils are likely to be recruited by mast cells in a positive feedback mechanism. Our data are in line with previous results showing mast cells to be essential for elevated TNF-α levels and neutrophil recruitment (Malaviya et al., 1996; Sun et al., 2007). TNF-α also has been implicated in MCP-1 production (Murao et al., 2000), relevant for monocyte recruitment (Ito et al., 1997). In our study, boosting mast cell activation by C48/80 resulted in increased levels of macrophages and T cells, particularly at day 3 after fal. Recruitment of perivascular macrophages supplying growth factors to growing blood vessels (Arras et al., 1998) was demonstrated to be essential for arteriogenesis (Heil et al., 2002; Hoefer et al., 2004; Ito et al., 1997), whereas T cells have been described to contribute to macrophage recruitment (Stabile et al., 2003). Hence, mast cells indirectly promoted arteriogenesis by amplifying the inflammatory reaction, thus providing macrophage-derived growth factors supporting vascular cell proliferation. In addition, mast cells may directly contribute to vascular cell proliferation as shown by our in vitro results.

In a more translational approach, we administrated dipA, which again increased perfusion recovery. Platelets, which transiently adhere to the endothelium of growing collaterals in the early phase of arteriogenesis (Chandraratne et al., 2015), are a rich source of SDF-1α. Platelet activation enhances surface expression and release of SDF-1α (Chatterjee and Gawaz, 2013), which results in recruitment of CXCR-4$^+$ cells at the site of inflammation. The administration of dipA, blocking DPPIV activity and, hence, SDF-1α degradation, resulted in a drastic increase in the number of c-kit$^+$ mast cells together with a significantly improved perfusion recovery.

Combined treatment of mice with C48/80 and dipA showed additive effects in terms of perfusion recovery and leukocyte recruitment, and it protected tissue from severe ischemic damage by effectively promoting arteriogenesis. Although we found that leukocytes, which express the SDF-1α receptor CXCR-4 as well, are recruited upon dipA treatment, a substantial increase in leukocyte recruitment occurred not earlier than upon treatment with dipA in combination with C48/80 (Figure 2D), arguing for the relevance of mast cells in this process.

Mast cells express the SDF-1α receptor CXCR-4 as well as the SCF receptor c-kit. Both ligands have been addressed in many experimental as well as clinical settings to recruit stem cells aiming at promoting neovascularization. Since it has been demonstrated previously that bone marrow-derived stem cells do not differentiate to ECs or SMCs and, hence, do not contribute to vascularization, i.e., arteriogenesis and angiogenesis (Ziegelhoeffer et al., 2004), our results may shed a different light on the nature of c-kit$^+$/CXCR-4$^+$ stem cells recruited to sites of neovascularization. Diverse studies could not demonstrate the presence of recruited stem cells at sites of (neo-) vascularization despite a functional improvement. In this context it might be of particular interest to mention that extensively degranulated mast cells cannot be identified anymore as individual cells in tissue (McGowen et al., 2009). A huge number of publications are available attributing mast cells an essential role in tumor angiogenesis; however, little information is available on the role of mast cells under other pathological or physiological conditions and results are contradictory.

Much effort has been made to find new therapeutic options to treat patients with vascular occlusive diseases. Here we show that promoting mast cell recruitment concomitant with mast cell activation promotes the growth of natural arteriolar bypasses to such an extent that distal tissue is preserved from severe ischemic damage. Local administration of C48/80 showed no systemic side effects in our study, and mast cell activators as well as drugs that inhibit DPPIV are used in clinical applications (Rukwied et al., 2000; Yanai, 2014). Recent clinical studies showed no major adverse cardiovascular events in patients with type 2 diabetes treated with DPPIV inhibitors

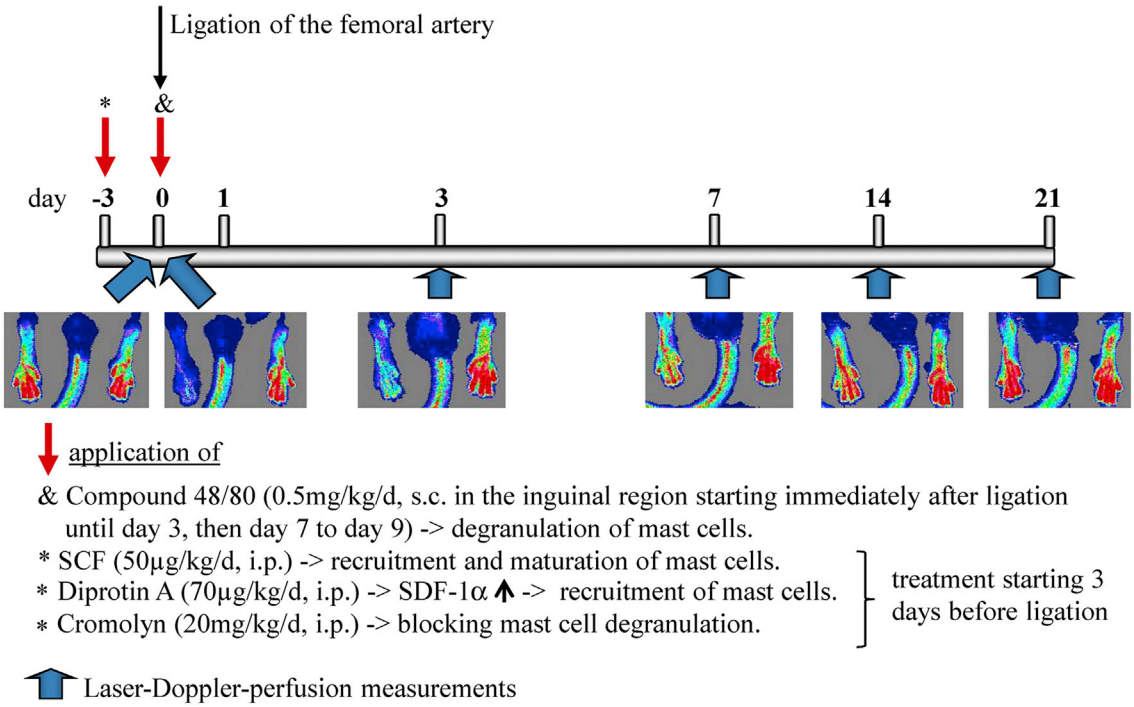

Figure 7. Study Protocol

Treatment protocol of mice with C48/80, SCF, dipA, or cromolyn with the indicated time points of laser Doppler perfusion measurements. Tissue for qRT-PCR was harvested at 12 hr, for protein analyses at 24 hr, for flow cytometry analyses at days 1 and 3, and for histology or immunohistology at 2 hr, 12 hr, 24 hr, 3 days, or 7 days after fal (right leg) or sham operation (left leg).

(White et al., 2013) and evidenced a lower risk for hospitalization for heart failure (Fadini et al., 2015), although there might be differences depending on the DPPIV inhibitor used. Therefore, SDF-1α, which recently has been shown in an animal model to promote vascular outward remodeling when locally released (Krieger et al., 2016), or DPPIV inhibitors alone or in combination with locally applied mast cell-activating factors may represent therapeutic approaches to treat affected patients non-invasively.

Collectively, our data show that mast cells play a central role in arteriogenesis by converting signals derived from upstream platelets and neutrophils in actions that specifically support the process of collateral artery growth. Pharmacological induction of mast cell recruitment and degranulation effectively promotes arteriogenesis, thereby protecting tissue from severe ischemic damage, and may thus constitute a therapeutic approach to treat patients with vascular occlusive diseases.

EXPERIMENTAL PROCEDURES

Murine Hindlimb Model of Arteriogenesis and Bone Marrow Transplantation

Animal care and all experimental procedures were performed in strict accordance to the German and NIH animal legislation guidelines and were approved by the Bavarian Animal Care and Use Committee (GZ. 55.2-1-54-2532-73-12). Ligation of the right femoral artery was induced in 8- to 10-week-old male SV129/S6 mice (Charles River Laboratories) treated with the indicated substances (for protocol see Figure 7 and the Supplemental Experimental Procedures); in bone marrow-transplanted mice; in Mcpt5-Cre^{+} R-DTA, Nox2−/−, uPA−/−, and IL4-R/Iba mice; and in corresponding wild-type littermates, respectively, as previously described (Limbourg et al., 2009). The left side was sham operated and served as control. For Laser-Doppler perfusion measurements, bone marrow transplantation, and further information, see the Supplemental Experimental Procedures.

SDF-1α, TNF-α, and MCP-1 Quantifications

SDF-1α protein levels in serum and collaterals were analyzed using a mouse SDF-1α ELISA kit (ELM-SDF1alpha-001-1, RayBiotech). MCP-1 and TNF-α protein levels were analyzed with MCP-1 and TNF-α ELISA ready-SET-go (REF 88-7391-22 and REF 88-7324-88, eBioscience), respectively, following the manufacturer's protocol. Plasma was collected from heparinized blood after centrifugation at 2,300 × *g* at 4°C for 20 min. Tissue was homogenized with 200 µl of cell lysis buffer (25 mM Tris [pH 7.5], 1% Triton X-100, 0.5 mM EDTA, 150 mM NaCl, 10 mM NaF, and 1% PMSF), treated five times for 2 s with ultrasound, and centrifuged as described above. For qRT-PCR analyses of MCP-1, see the Supplemental Experimental Procedures.

MMP Activity Assay

MMP activity in collateral samples was analyzed with SensoLyte 520 Generic MMP Assay Kit (Anaspec). Briefly, collaterals were homogenized in assay buffer with 0.1% (v/v) Triton X-100, centrifuged, and supernatants were incubated for 2 hr with 4-aminophenylmercuric acetate (APMA) at 37°C, following the manufacturer's protocol. Fluorescence signal was measured at excitation/emission = 490/520 nm for 1 hr (Infinite 200, S/N 711003634, TECAN). Data were normalized to the reference standard curve.

Histology and Immunohistology

Paraffin-embedded issue samples were isolated at the indicated time points. After deparaffinization and antigen retrieval using Target Retrieval Solution

(S1699, Dako), sections were stained for CD31 (DIA-310, Dianova, dilution 1:150), Ki67 (M7249, Dako, dilution 1:100), or CD45 (550539, BD Pharmingen, dilution 1:600), respectively. For detection of the immunoreaction, the Vectastain ABC-Kit Elite Rat IgG (PK6104, Vector Laboratories) was used. DAB+ (K3468, Dako) served as chromogen for CD31 and ACE (00-1122, Invitrogen) for Ki67 and CD45 staining. Giemsa and H&E staining were performed according to standard procedures. The luminal diameter of collateral arterioles was measured in at least three different sites of an individual arteriole. Cryopreserved tissue samples were stained with an antibody against c-kit (14-1172-85, eBioscience, dilution 1:100) and secondary antibody donkey anti-rat Cy3 (AC189C, Millipore, dilution 1:300); FGF-2 (ab106245, Abcam, dilution 1:100) and secondary antibody donkey anti-rabbit AF488 (A21206, MoBiTec, dilution 1:100); or PDGF-BB (ab16829, Abcam, dilution 1:100) and secondary antibody donkey anti-rabbit AF488 (A21206, MoBiTec, dilution 1:100), respectively, and viewed with a confocal microscope (Leica SP5).

Flow Cytometry Analyses of Muscle Tissue

For flow cytometry analysis, adductor muscles were digested with 1 mg/ml collagenase II (Biochrom) in PBS/1% BSA at 37°C for 90 min. The suspension was then filtered with PBS/2% BSA through a 70-μm cell strainer (BD Falcon), spun for 10 min at 160 × *g*, and the pellet was finally resuspended in 100 μl PBS/2% BSA. Surface staining was conducted using CD 45 rat anti-mouse APC-Cy7 (557659, clone 30-F11, BD Biosciences), F4/80 rat anti-mouse eFluor 450 (48-4801, clone BM8, eBioscience), CD 115 rat anti-mouse APC (17-1152, clone AFS98, eBioscience), CD 11b rat anti-mouse fluorescein isothiocyanate (FITC) (11-0112, clone m1/70, eBioscience), GR-1 rat anti-mouse PE (553128, clone RB6-8C5, BD Biosciences), c-kit (CD117) rat anti-mouse PerCP/Cy5.5 (105823, clone 2B8, BioLegend), and CD3 rat anti-mouse eFlour 450 (48-0032, clone 17A2, eBioscience). Rat isotype controls were as follows: IgG2b APC-Cy7 (552773, clone A95-1, BD Biosciences), IgG2a eFluor 450 (48-4321, clone eBR2a, eBioscience), IgG2a APC (17-4321, clone eBR2a, eBioscience), IgG 1 FITC (11-4301, clone eBRG1, eBioscience), IgG2b PE (553989, clone A95-1, BD Biosciences), and IgG2a PerCP/Cy5.5 (45-4321, clone eBR2a, eBioscience). Becton Dickinson fluorescence-activated cell sorting (FACS) lysing solution was used to fix and lyse the samples according to the manufacturer's protocol. Samples were measured using Gallios flow cytometer and analyzed with Kaluza Software (both from Beckman Coulter Genomics).

In Vitro Analyses

For protocols of the in vitro analyses, see the Supplemental Experimental Procedures.

Statistical Analysis

Comparisons between groups were calculated by unpaired Student's t test unless otherwise stated. Results were considered to be statistically significant at $^*p \leq 0.05$. Data are represented as means ± SEM. Statistical analyses were performed with GraphPad software PRISM6.

SUPPLEMENTAL INFORMATION

Supplemental Information includes Supplemental Experimental Procedures and seven figures and can be found with this article online at http://dx.doi.org/10.1016/j.celrep.2016.07.040.

AUTHOR CONTRIBUTIONS

O.C., E.C.K., T.L., J.-I.P., M.R., and M.L. performed in vivo measurements and histological analyses. Y.H. and H.M. conducted in vitro analyses on platelets and neutrophils. A.C.-M. and S.F. performed qRT-PCR, MMP activity assay, and protein analyses. A.M. conducted in vitro proliferation assays, K.T. performed immunohistology, and A.R.M.K. helped with FACS analyses. G.A. helped with histology data analysis. S.M.K., B.N., B.W., C.A.R., and K.T.P. participated in scientific discussions and drafting of the manuscript. E.D. performed experimental design, data analysis, conducted scientific direction, and wrote the manuscript.

ACKNOWLEDGMENTS

This work was supported by the Fritz-Bender-Stiftung (E.D.), the Deutscher Akademischer Austauschdienst (DAAD) (E.D.), the Münchener Universitätsgesellschaft (E.D.), the v. Behring-Röntgen-Foundation (S.F. and K.T.P.), and the Deutsche Forschungsgemeinschaft (SFB 914/TP A02 [B.W.] and /TP B03 [C.A.R.]). The authors are thankful to N. Weissmann, Justus-Liebig-University, for the Nox2−/− mice; S. Massberg, Ludwig-Maximilians-University, for IL4-R/Iba mice; D. Vestweber, Max Planck Institute for Molecular Biomedicine, for PSGL-1−/− and P-selectin −/− mice; A. Roers for Mcpt5-Cre R-DTA mice; and C. Csapo, M.-P. Wu, J. Truong, S. Tannert Otto, S. Schaefer, A. Heier, A. Sendelthofer, and Tobias Haering for technical assistance.

Received: December 25, 2015
Revised: June 23, 2016
Accepted: July 17, 2016
Published: August 11, 2016

REFERENCES

Arras, M., Ito, W.D., Scholz, D., Winkler, B., Schaper, J., and Schaper, W. (1998). Monocyte activation in angiogenesis and collateral growth in the rabbit hindlimb. J. Clin. Invest. *101*, 40–50.

Cai, W., Vosschulte, R., Afsah-Hedjri, A., Koltai, S., Kocsis, E., Scholz, D., Kostin, S., Schaper, W., and Schaper, J. (2000). Altered balance between extracellular proteolysis and antiproteolysis is associated with adaptive coronary arteriogenesis. J. Mol. Cell. Cardiol. *32*, 997–1011.

Cao, R., Bråkenhielm, E., Pawliuk, R., Wariaro, D., Post, M.J., Wahlberg, E., Leboulch, P., and Cao, Y. (2003). Angiogenic synergism, vascular stability and improvement of hind-limb ischemia by a combination of PDGF-BB and FGF-2. Nat. Med. *9*, 604–613.

Chandraratne, S., von Bruehl, M.L., Pagel, J.I., Stark, K., Kleinert, E., Konrad, I., Farschtschi, S., Coletti, R., Gärtner, F., Chillo, O., et al. (2015). Critical role of platelet glycoprotein ibα in arterial remodeling. Arterioscler. Thromb. Vasc. Biol. *35*, 589–597.

Chang, J.C., Leung, J., Tang, T., Holzknecht, Z.E., Hartwig, M.G., Duane Davis, R., Parker, W., Abraham, S.N., and Lin, S.S. (2014). Cromolyn ameliorates acute and chronic injury in a rat lung transplant model. Journal Heart Lung Transplant. *33*, 749–757.

Chatterjee, M., and Gawaz, M. (2013). Platelet-derived CXCL12 (SDF-1α): basic mechanisms and clinical implications. J. Thromb. Haemost. *11*, 1954–1967.

Deindl, E., and Schaper, W. (2005). The art of arteriogenesis. Cell Biochem. Biophys. *43*, 1–15.

Deindl, E., Ziegelhöffer, T., Kanse, S.M., Fernandez, B., Neubauer, E., Carmeliet, P., Preissner, K.T., and Schaper, W. (2003). Receptor-independent role of the urokinase-type plasminogen activator during arteriogenesis. FASEB J. *17*, 1174–1176.

Egashira, Y., Suzuki, Y., Azuma, Y., Takagi, T., Mishiro, K., Sugitani, S., Tsuruma, K., Shimazawa, M., Yoshimura, S., Kashimata, M., et al. (2013). The growth factor progranulin attenuates neuronal injury induced by cerebral ischemia-reperfusion through the suppression of neutrophil recruitment. J. Neuroinflammation *10*, 105.

Fadini, G.P., Avogaro, A., Degli Esposti, L., Russo, P., Saragoni, S., Buda, S., Rosano, G., Pecorelli, S., and Pani, L.; OsMed Health-DB Network (2015). Risk of hospitalization for heart failure in patients with type 2 diabetes newly treated with DPP-4 inhibitors or other oral glucose-lowering medications: a retrospective registry study on 127,555 patients from the Nationwide OsMed Health-DB Database. Eur. Heart J. *36*, 2454–2462.

Gan, X., Xing, D., Su, G., Li, S., Luo, C., Irwin, M.G., Xia, Z., Li, H., and Hei, Z. (2015). Propofol attenuates small intestinal ischemia reperfusion injury through inhibiting NADPH oxidase mediated mast cell activation. Oxid. Med. Cell. Longev. *2015*, 167014.

Griffin, G.K., Newton, G., Tarrio, M.L., Bu, D.X., Maganto-Garcia, E., Azcutia, V., Alcaide, P., Grabie, N., Luscinskas, F.W., Croce, K.J., and Lichtman,

A.H. (2012). IL-17 and TNF-α sustain neutrophil recruitment during inflammation through synergistic effects on endothelial activation. J. Immunol. *188*, 6287–6299.

Grundmann, S., Hoefer, I., Ulusans, S., van Royen, N., Schirmer, S.H., Ozaki, C.K., Bode, C., Piek, J.J., and Buschmann, I. (2005). Anti-tumor necrosis factor-alpha therapies attenuate adaptive arteriogenesis in the rabbit. Am. J. Physiol. Heart Circ. Physiol. *289*, H1497–H1505.

Heil, M., Ziegelhoeffer, T., Pipp, F., Kostin, S., Martin, S., Clauss, M., and Schaper, W. (2002). Blood monocyte concentration is critical for enhancement of collateral artery growth. Am. J. Physiol. Heart Circ. Physiol. *283*, H2411–H2419.

Hiromatsu, Y., and Toda, S. (2003). Mast cells and angiogenesis. Microsc. Res. Tech. *60*, 64–69.

Hoefer, I.E., van Royen, N., Rectenwald, J.E., Deindl, E., Hua, J., Jost, M., Grundmann, S., Voskuil, M., Ozaki, C.K., Piek, J.J., and Buschmann, I.R. (2004). Arteriogenesis proceeds via ICAM-1/Mac-1- mediated mechanisms. Circ. Res. *94*, 1179–1185.

Ito, W.D., Arras, M., Winkler, B., Scholz, D., Schaper, J., and Schaper, W. (1997). Monocyte chemotactic protein-1 increases collateral and peripheral conductance after femoral artery occlusion. Circ. Res. *80*, 829–837.

Köhler, D., Straub, A., Weissmüller, T., Faigle, M., Bender, S., Lehmann, R., Wendel, H.P., Kurz, J., Walter, U., Zacharowski, K., and Rosenberger, P. (2011). Phosphorylation of vasodilator-stimulated phosphoprotein prevents platelet-neutrophil complex formation and dampens myocardial ischemia-reperfusion injury. Circulation *123*, 2579–2590.

Kovanen, P.T. (2007). Mast cells: multipotent local effector cells in atherothrombosis. Immunol. Rev. *217*, 105–122.

Krieger, J.R., Ogle, M.E., McFaline-Figueroa, J., Segar, C.E., Temenoff, J.S., and Botchwey, E.A. (2016). Spatially localized recruitment of anti-inflammatory monocytes by SDF-1α-releasing hydrogels enhances microvascular network remodeling. Biomaterials *77*, 280–290.

Limbourg, A., Korff, T., Napp, L.C., Schaper, W., Drexler, H., and Limbourg, F.P. (2009). Evaluation of postnatal arteriogenesis and angiogenesis in a mouse model of hind-limb ischemia. Nat. Protoc. *4*, 1737–1746.

Maggi, L., Capone, M., Giudici, F., Santarlasci, V., Querci, V., Liotta, F., Ficari, F., Maggi, E., Tonelli, F., Annunziato, F., and Cosmi, L. (2013). CD4+CD161+ T lymphocytes infiltrate Crohn's disease-associated perianal fistulas and are reduced by anti-TNF-α local therapy. Int. Arch. Allergy Immunol. *161*, 81–86.

Malaviya, R., Ikeda, T., Ross, E., and Abraham, S.N. (1996). Mast cell modulation of neutrophil influx and bacterial clearance at sites of infection through TNF-alpha. Nature *381*, 77–80.

McGowen, A.L., Hale, L.P., Shelburne, C.P., Abraham, S.N., and Staats, H.F. (2009). The mast cell activator compound 48/80 is safe and effective when used as an adjuvant for intradermal immunization with Bacillus anthracis protective antigen. Vaccine *27*, 3544–3552.

Murao, K., Ohyama, T., Imachi, H., Ishida, T., Cao, W.M., Namihira, H., Sato, M., Wong, N.C., and Takahara, J. (2000). TNF-alpha stimulation of MCP-1 expression is mediated by the Akt/PKB signal transduction pathway in vascular endothelial cells. Biochem. Biophys. Res. Commun. *276*, 791–796.

Oliveira, S.H., and Lukacs, N.W. (2003). Stem cell factor: a hemopoietic cytokine with important targets in asthma. Curr. Drug Targets Inflamm. Allergy *2*, 313–318.

Page, C., and Pitchford, S. (2013). Neutrophil and platelet complexes and their relevance to neutrophil recruitment and activation. Int. Immunopharmacol. *17*, 1176–1184.

Pipp, F., Boehm, S., Cai, W.J., Adili, F., Ziegler, B., Karanovic, G., Ritter, R., Balzer, J., Scheler, C., Schaper, W., and Schmitz-Rixen, T. (2004). Elevated fluid shear stress enhances postocclusive collateral artery growth and gene expression in the pig hind limb. Arterioscler. Thromb. Vasc. Biol. *24*, 1664–1668.

Rao, K.N., and Brown, M.A. (2008). Mast cells: multifaceted immune cells with diverse roles in health and disease. Ann. N Y Acad. Sci. *1143*, 83–104.

Reichel, C.A., Uhl, B., Lerchenberger, M., Puhr-Westerheide, D., Rehberg, M., Liebl, J., Khandoga, A., Schmalix, W., Zahler, S., Deindl, E., et al. (2011). Urokinase-type plasminogen activator promotes paracellular transmigration of neutrophils via Mac-1, but independently of urokinase-type plasminogen activator receptor. Circulation *124*, 1848–1859.

Rudijanto, A. (2007). The role of vascular smooth muscle cells on the pathogenesis of atherosclerosis. Acta Med. Indones. *39*, 86–93.

Rukwied, R., Lischetzki, G., McGlone, F., Heyer, G., and Schmelz, M. (2000). Mast cell mediators other than histamine induce pruritus in atopic dermatitis patients: a dermal microdialysis study. Br. J. Dermatol. *142*, 1114–1120.

Sadler, J.E. (2002). A new name in thrombosis, ADAMTS13. Proc. Natl. Acad. Sci. USA *99*, 11552–11554.

Schulz, R., Murzabekova, G., Egemnazarov, B., Kraut, S., Eisele, H.J., Dumitrascu, R., Heitmann, J., Seimetz, M., Witzenrath, M., Ghofrani, H.A., et al. (2014). Arterial hypertension in a murine model of sleep apnea: role of NADPH oxidase 2. J. Hypertens. *32*, 300–305.

Stabile, E., Burnett, M.S., Watkins, C., Kinnaird, T., Bachis, A., la Sala, A., Miller, J.M., Shou, M., Epstein, S.E., and Fuchs, S. (2003). Impaired arteriogenic response to acute hindlimb ischemia in CD4-knockout mice. Circulation *108*, 205–210.

Stabile, E., Kinnaird, T., la Sala, A., Hanson, S.K., Watkins, C., Campia, U., Shou, M., Zbinden, S., Fuchs, S., Kornfeld, H., et al. (2006). CD8+ T lymphocytes regulate the arteriogenic response to ischemia by infiltrating the site of collateral vessel development and recruiting CD4+ mononuclear cells through the expression of interleukin-16. Circulation *113*, 118–124.

Sun, J., Sukhova, G.K., Wolters, P.J., Yang, M., Kitamoto, S., Libby, P., MacFarlane, L.A., Mallen-St Clair, J., and Shi, G.P. (2007). Mast cells promote atherosclerosis by releasing proinflammatory cytokines. Nat. Med. *13*, 719–724.

Tobar, N., Villar, V., and Santibanez, J.F. (2010). ROS-NFkappaB mediates TGF-beta1-induced expression of urokinase-type plasminogen activator, matrix metalloproteinase-9 and cell invasion. Mol. Cell. Biochem. *340*, 195–202.

Weber, F.C., Nemeth, T., Csepregi, J.Z., Dudeck, A., Roers, A., Ozsvari, B., Oswald, E., Puskas, L.G., Jakob, T., Mocsai, A., and Martin, S.F. (2015). Neutrophils are required for both the sensitization and elicitation phase of contact hypersensitivity. J. Exp. Med. *212*, 15–22.

White, W.B., Cannon, C.P., Heller, S.R., Nissen, S.E., Bergenstal, R.M., Bakris, G.L., Perez, A.T., Fleck, P.R., Mehta, C.R., Kupfer, S., et al.; EXAMINE Investigators (2013). Alogliptin after acute coronary syndrome in patients with type 2 diabetes. N. Engl. J. Med. *369*, 1327–1335.

Wolf, C., Cai, W.J., Vosschulte, R., Koltai, S., Mousavipour, D., Scholz, D., Afsah-Hedjri, A., Schaper, W., and Schaper, J. (1998). Vascular remodeling and altered protein expression during growth of coronary collateral arteries. J. Mol. Cell. Cardiol. *30*, 2291–2305.

Yanai, H. (2014). Dipeptidyl peptidase-4 inhibitor sitagliptin significantly reduced hepatitis C virus replication in a diabetic patient with chronic hepatitis C virus infection. Hepatobiliary Pancreat. Dis. Int. *13*, 556.

Yang, M.Q., Ma, Y.Y., Tao, S.F., Ding, J., Rao, L.H., Jiang, H., and Li, J.Y. (2014). Mast cell degranulation promotes ischemia-reperfusion injury in rat liver. J. Surg. Res. *186*, 170–178.

Zaruba, M.M., Theiss, H.D., Vallaster, M., Mehl, U., Brunner, S., David, R., Fischer, R., Krieg, L., Hirsch, E., Huber, B., et al. (2009). Synergy between CD26/DPP-IV inhibition and G-CSF improves cardiac function after acute myocardial infarction. Cell Stem Cell *4*, 313–323.

Ziegelhoeffer, T., Fernandez, B., Kostin, S., Heil, M., Voswinckel, R., Helisch, A., and Schaper, W. (2004). Bone marrow-derived cells do not incorporate into the adult growing vasculature. Circ. Res. *94*, 230–238.

Cell Reports, Volume *16*

Supplemental Information

Perivascular Mast Cells Govern Shear Stress-Induced Arteriogenesis by Orchestrating Leukocyte Function

Omary Chillo, Eike Christian Kleinert, Thomas Lautz, Manuel Lasch, Judith-Irina Pagel, Yvonn Heun, Kerstin Troidl, Silvia Fischer, Amelia Caballero-Martinez, Annika Mauer, Angela R.M. Kurz, Gerald Assmann, Markus Rehberg, Sandip M. Kanse, Bernhard Nieswandt, Barbara Walzog, Christoph A. Reichel, Hanna Mannell, Klaus T. Preissner, and Elisabeth Deindl

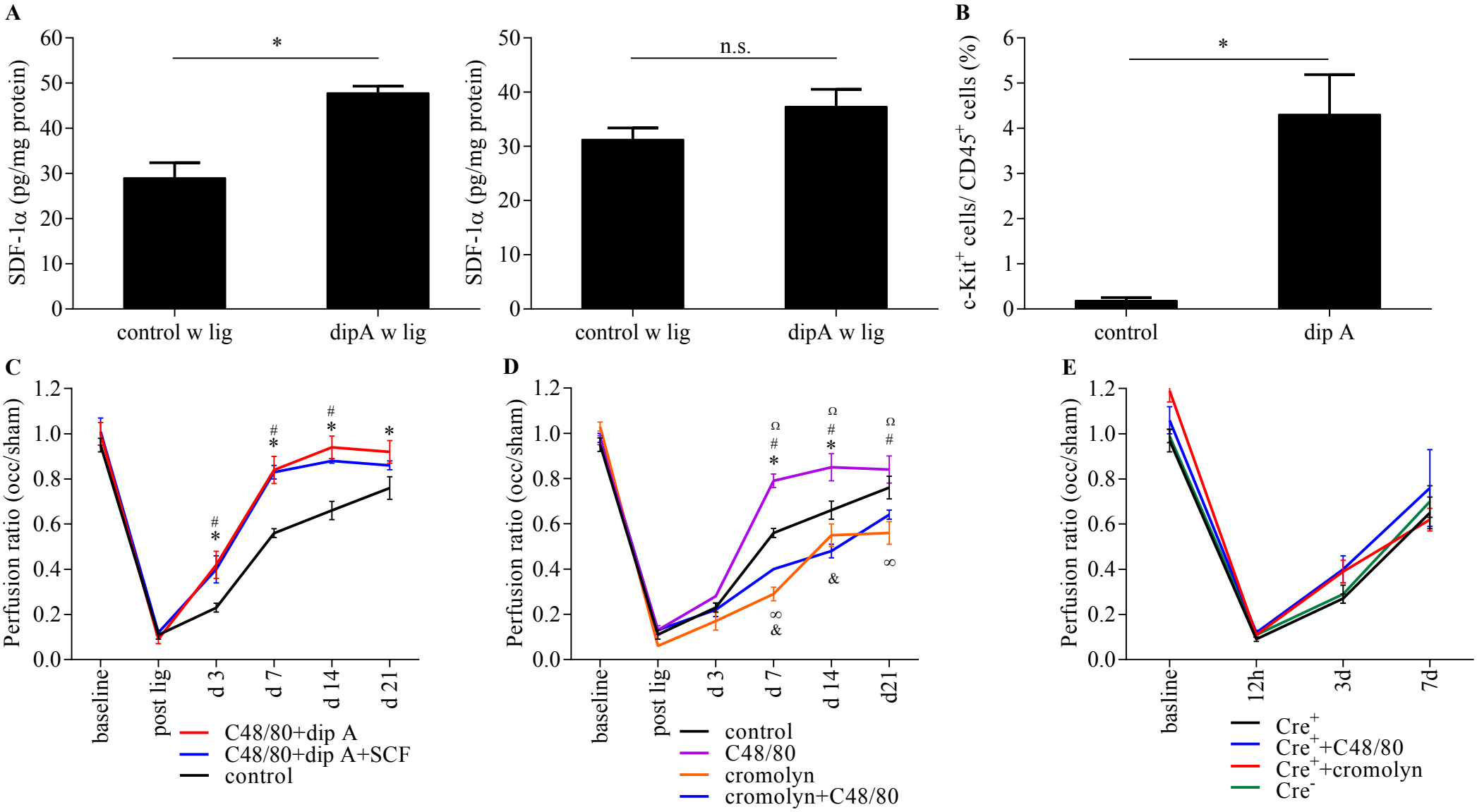

Figure S1. Related to Figure 1. Pharmaceutical recruitment and activation of mast cells promotes arteriogenesis

(A) SDF-1α levels were measured to investigate the effectiveness of diprotin A treatment. The SDF-1α levels in collateral arteries (left panel) or sera (right panel) of mice isolated 24h after fal and saline treatment (control w lig), or 24h after fal and diprotin A treatment (dipA w lig) were assessed by ELISA. n=3 in triplicates. (B) Flow cytometry analyses of CD45+/c-kit+ cells in adductor muscles of mice at day 1 after fal and saline (control) or dipA treatment. n=6. (C, D, E) Laser Doppler perfusion measurements following fal (right leg) and sham operation (left leg). Color-coded lines indicate treatment of mice (control = saline). Statistical analysis ($P < 0.05$) was performed between different groups (n=6 per group) using repeated measures two-way ANOVA with subsequent multiple comparisons by Bonferroni test. (C) Treatment of mice with C48/80+dipA+SCF showed no additive effects compared to C48/80+dipA treatment. The control and internal control (C48/80+dipA) are identical to Figure 1D. *C48/80+dipA vs control; #C48/80+dipA+SCF vs control. (D) Cromolyn treatment abolished the positive effect of C48/80. The control and internal controls (C48/80, cromolyn) are identical to Figure 1D. *C48/80 vs control; #C48/80 vs cromolyn; ΩC48/80 vs cromolyn+C48/80; ∞cromolyn vs control; &cromolyn+C48/80 vs control. (E) Perfusion recovery of mast cell deficient Mcpt5-Cre+ R-DTA mice (Cre+) was neither influenced by C48/80 treatment nor by cromolyn treatment. Control mice: Cre-. Data are means ± SEM.

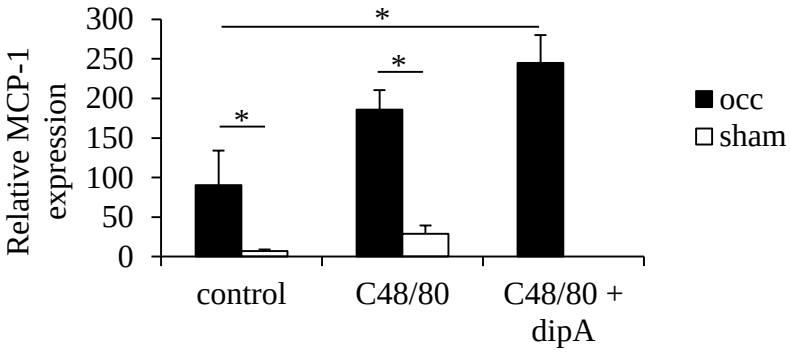

Figure S2. Related to Figure 2. MCP-1 mRNA levels

mRNA expression level of MCP-1 in collaterals of mice treated with saline (control), C48/80, or C48/80 and dipA (C48/80+dipA), 12h after fal (occ) or sham operation, as measured by qRT-PCR. Data are means ± SEM; n=3 in triplicates. Statistical significances (*P ≤ 0.05) are from two-way ANOVA with subsequent Newman-Keuls test.

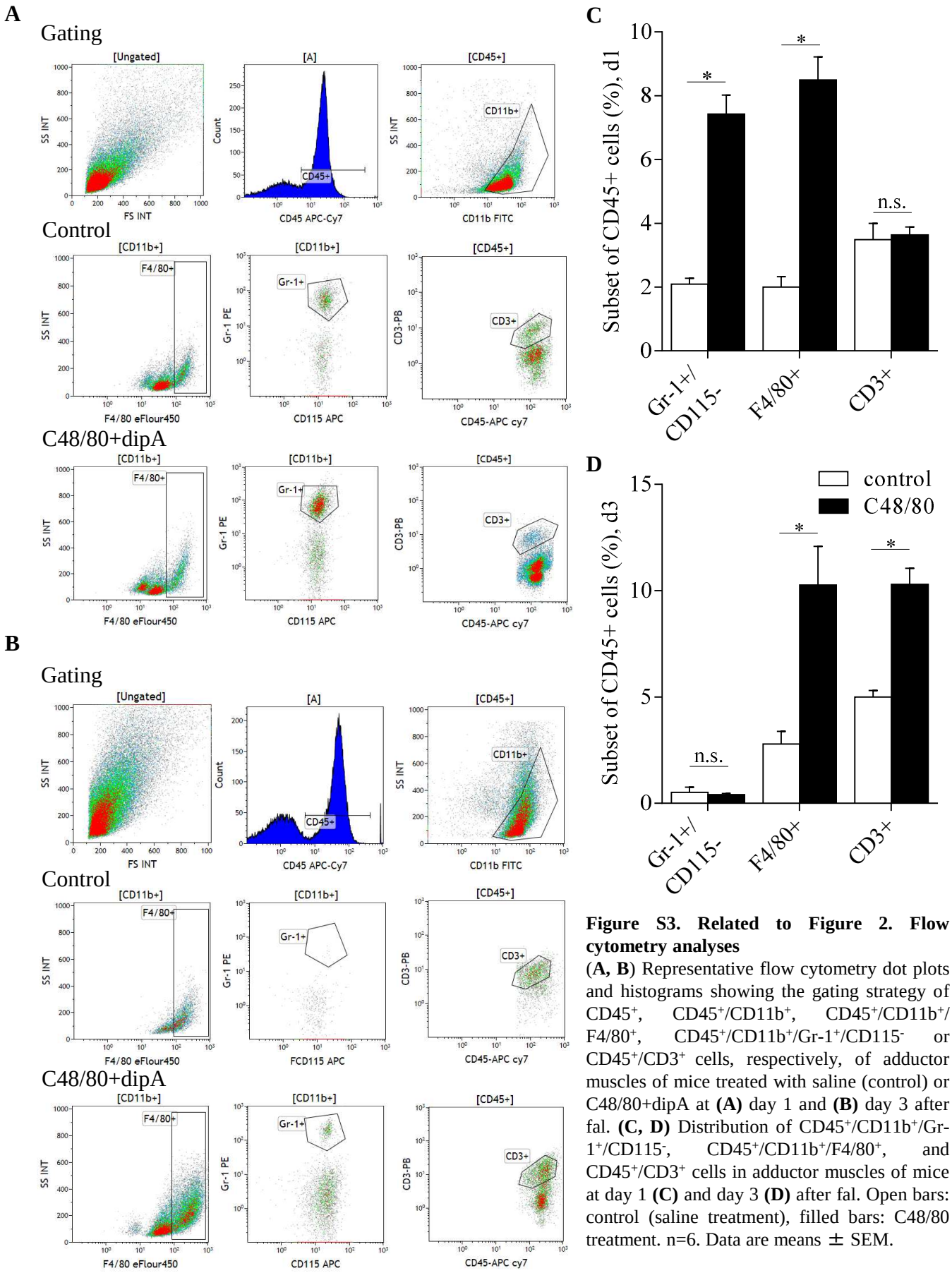

Figure S3. Related to Figure 2. Flow cytometry analyses

(**A, B**) Representative flow cytometry dot plots and histograms showing the gating strategy of $CD45^+$, $CD45^+/CD11b^+$, $CD45^+/CD11b^+/F4/80^+$, $CD45^+/CD11b^+/Gr\text{-}1^+/CD115^-$ or $CD45^+/CD3^+$ cells, respectively, of adductor muscles of mice treated with saline (control) or C48/80+dipA at **(A)** day 1 and **(B)** day 3 after fal. **(C, D)** Distribution of $CD45^+/CD11b^+/Gr\text{-}1^+/CD115^-$, $CD45^+/CD11b^+/F4/80^+$, and $CD45^+/CD3^+$ cells in adductor muscles of mice at day 1 **(C)** and day 3 **(D)** after fal. Open bars: control (saline treatment), filled bars: C48/80 treatment. n=6. Data are means ± SEM.

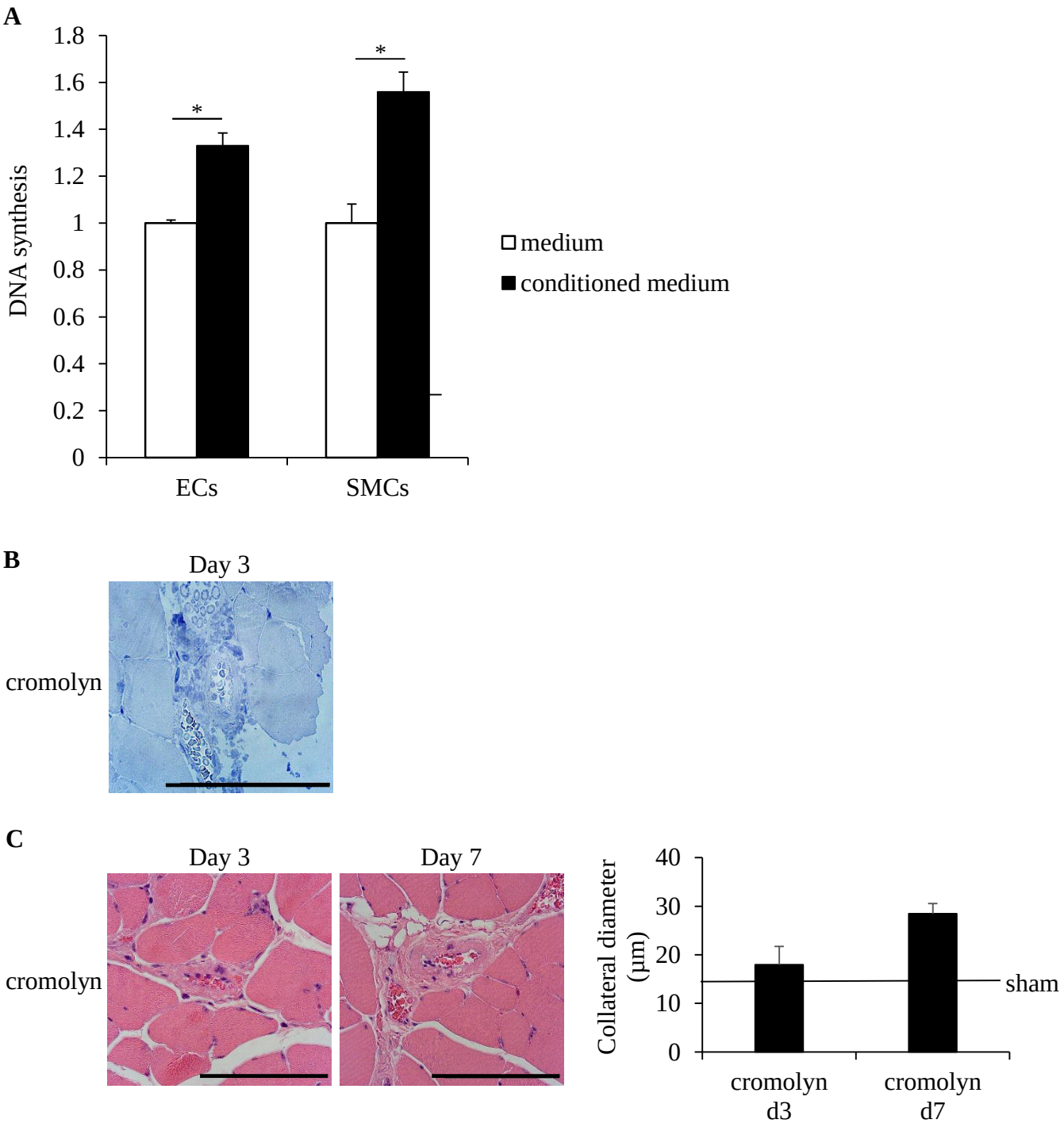

Figure S4. Related to Figure 3. In vitro proliferation assay and histological analyses

(**A**) Influence of mast cell degranulation factors on in vitro proliferation of primary murine endothelial (ECs) and smooth muscle cells (SMCs), measured by detection of DNA synthesis. Medium: supernatant of mast cells without induction of degranulation (control, number was defined as 1); conditioned medium: supernatant of degranulated mast cells. Data are means ± SEM; n=3 in triplicates. (**B**) Immuno-staining of cromolyn treated mice showed no $Ki67^{+}$ cells (stained in brown) in collaterals of mice 3 days after fal. Scale bar = 100mm. (**C**) Left: representative images of HE staining of collaterals of mice treated with cromolyn at day 3 or day 7 after fal. Scale bar = 100mm. Right: for measurement of luminal diameter 3 animals with 3 collaterals each were analyzed. Data are means ± SEM

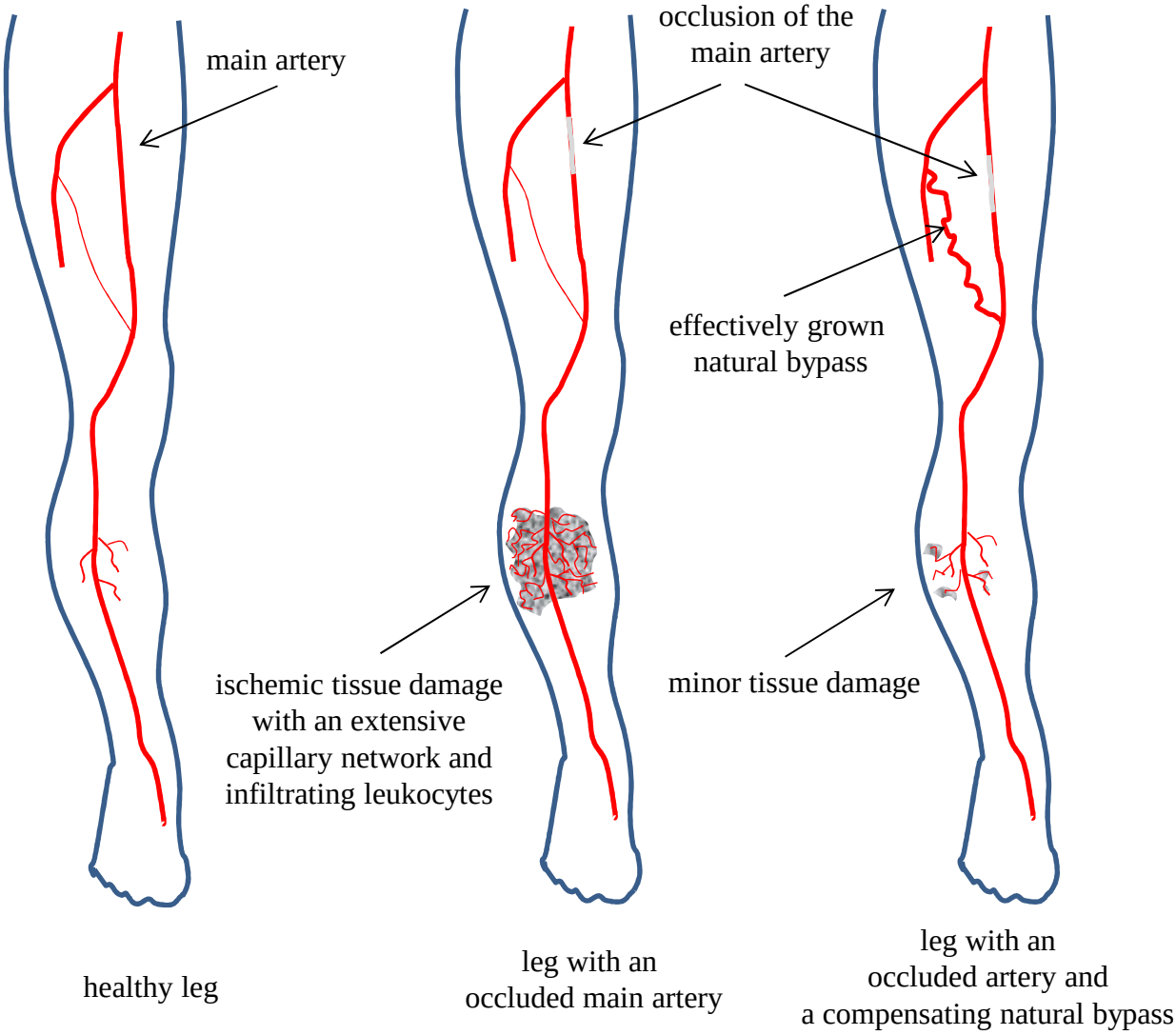

Figure S5. Related to Figure 4. Natural bypasses protect tissue from ischemic damage
Arteries have the function to transport oxygenated blood through the body. In the legs, the femoral artery of the upper leg is the main artery being responsible for blood supply to the lower leg (left). Upon occlusion of the femoral artery, the lower limb suffers from reduced blood supply resulting in tissue fibrosis and gangrene formation. This is associated with a strong infiltration of leukocytes and extensive capillary sprouting in order to remove cellular debris (middle). However, in case of effective collateral artery growth compensating for the loss of the occluded main artery, sufficient blood is transported to the lower leg by naturally grown bypasses preventing severe tissue damage. Accordingly, there is a reduced infiltration of leukocytes and capillary sprouting (right).

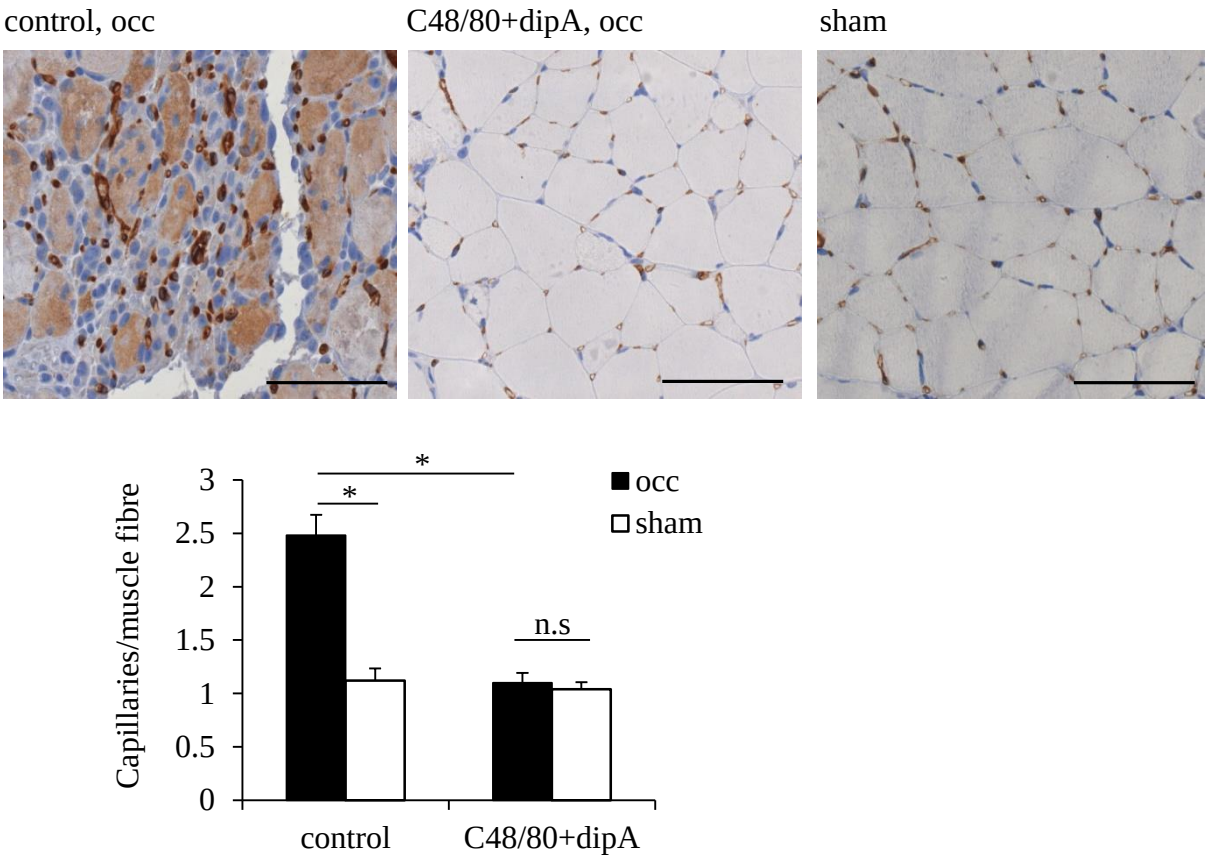

Figure S6. Related to Figure 4. Capillary/muscle fibre ratio

Upper panel: representative CD31 staining (ECs appear in brown) of the m. gastrocnemius of sham operated mice (sham) or mice treated with saline (control, occ) or C48/80+dipA (C48/80+dipA, occ) 3 days after fal. Scale bar = 100mm. Lower panel: for quantification of the capillary/muscle fibre ratio in gastrocnemius muscles high power fields of 6 slices from 3 individual experiments were analyzed. Data are means ± SEM. Significances are from two-way ANOVA with subsequent Newman-Keuls test.

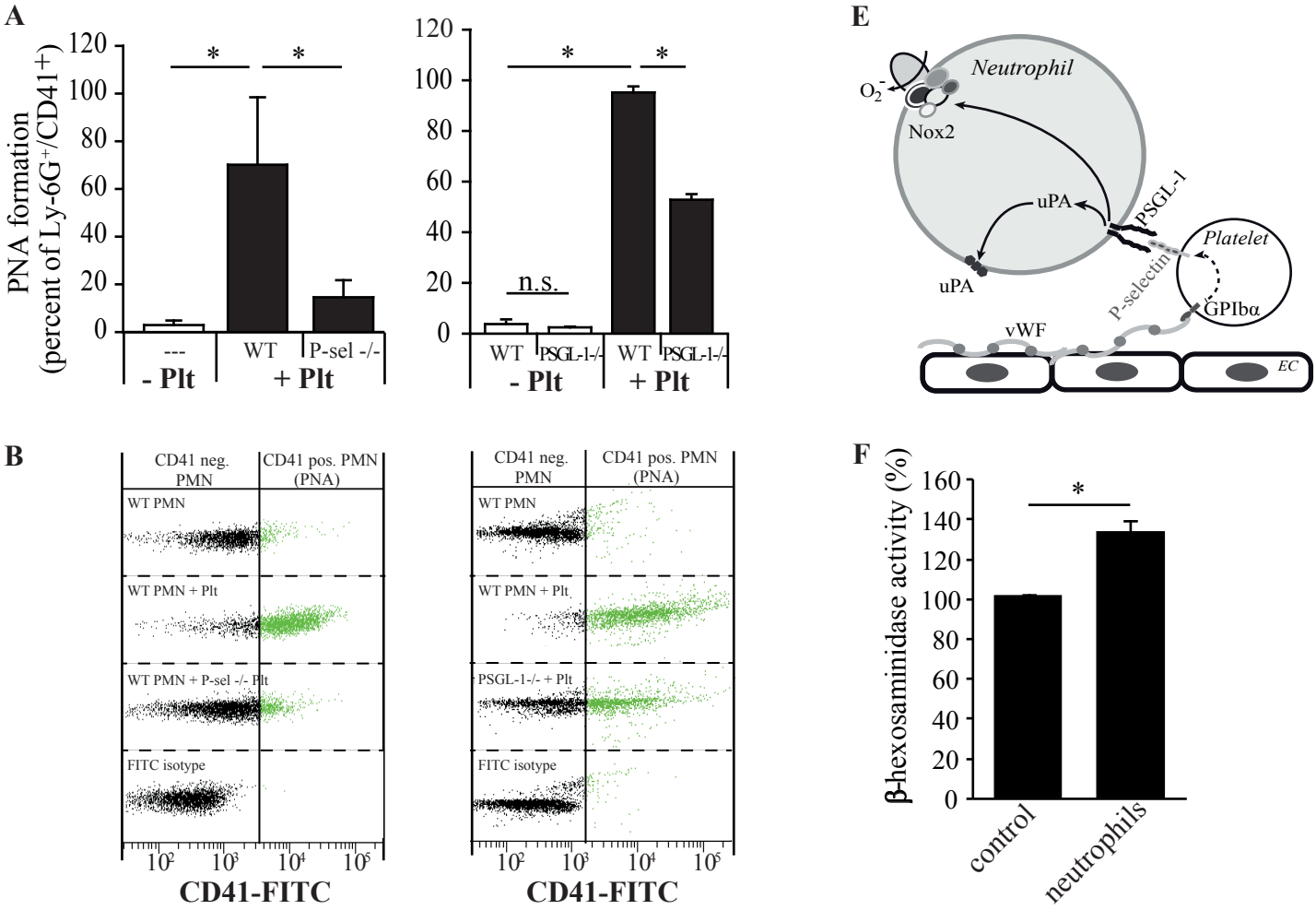

Figure S7. Related to Figure 5 and 6. Activation of neutrophils

(A) P-selectin deficient platelets as well as PSGL-1 deficient neutrophils showed reduced formation of platelet neutrophil aggregates (PNA) compared to wild type (WT) platelets (*P ≤ 0.05, (n=5 in duplicates) or WT neutrophils (n=3 in duplicates, *P ≤ 0.05), respectively, as measured with flow cytometry of Ly-6G+/CD41+ cells. (B) Representative flow cytometry dot plots of CD41 staining (green) in Ly-6G positive populations. (C) While PNA formation increased uPA surface expression on neutrophils (*P ≤ 0.05, n=5 in duplicates), as detected by flow cytometry, PSGL-1-/- neutrophils (*P ≤ 0.05, n=5 in duplicates) as well as P-selectin -/- platelets showed decreased uPA surface expression (*P ≤ 0.05, n=5 in duplicates). (D) PNA induced Nox2 derived extracellular superoxide formation (both *P ≤ 0.05, n=4 in duplicates), as assessed by the cytochrome C assay, was reduced when using P-selectin -/- platelets (*P ≤ 0.05, n=5 in duplicates). All data are presented as means ± SEM and considered significant at an error probability level of P ≤ 0.05. (E) Proposed model for neutrophil activation during arteriogenesis: Increased shear stress, triggering arteriogenesis (Pipp et al., 2004), induces vWF release from ECs, which binds to platelet GPIbα (Chandraratne et al., 2015; Sadler, 2002) resulting in surface expression of P-selectin on platelets (Goto et al., 2000). Subsequent PNA formation (Chandraratne et al., 2015) mediated by binding of platelet P-selectin to neutrophil PSGL-1 is associated with uPA release (Plesner et al., 1994) to the cell surface and initiates neutrophil extravasation together with EC uPA (Reichel et al., 2011). (F) Co-culture of mast cells and activated neutrophils increased β-hexosaminidase activity, indicative for mast cell degranulation. The activity of control mast cells was set to 100 %. (*P ≤ 0.05, n=3 in duplicates).

Supplemental Experimental Procedures

Murine hindlimb model of arteriogenesis
Ligation of the right femoral artery was induced in 8-10 weeks old mast cell deficient (Mcpt5-Cre$^+$ R-DTA) (Dudeck et al., 2011), GPIbα deficient (IL4-R/Iba mice) (Chandraratne et al., 2015), Nox2 deficient (Schulz et al., 2013), uPA deficient mice (Deindl et al., 2003) or corresponding wild type littermates as previously described (Limbourg et al., 2009). The left side was sham operated and served as control. SV129/S6 mice receiving the same surgical procedure were treated with Compound 48/80 to boost mast cell degranulation (McGowen et al., 2009), Diprotin A to boost mast cell recruitment (Juremalm et al., 2000; Zaruba et al., 2009), cromolyn to block mast cell degranulation (Vincent et al., 2013) (all from Sigma Aldrich) or SCF to boost mast cell maturation and activation (Oliveira and Lukacs, 2003) (Immuno Tools) as shown and described in Figure 7. 10µl of uPA inhibitor UK122 (150mg/kg dissolved in DMSO, i.v., Santa Cruz) or solvent was given 1h before fal. The GPIbα-inhibiting Fab fragment or the specific control isotype Fab (Chandraratne et al., 2015) was administered immediately before ligation (150mg/kg, i.v.). Apocynin (Schulz et al., 2013) (50mg/kg/d) (Santa Cruz Biotechnology) or N-acetylcysteine (Tobar et al., 2010) (1g/kg/d) (Sigma Aldrich), respectively, was administered in drinking water starting 3 days before ligation. Neutropenia was induced by administration of neutrophil depleting antibody 1A8 (Drechsler et al., 2010) (100mg/kg, i.p.) (BioXcell) 2 days before ligation and again immediately after fal. Blinded analysis was performed when evaluating tissue samples from these experiments.

Laser Doppler perfusion measurements
Laser Doppler perfusion measurements and calculations of left leg to right leg ratio were performed as previously described (Limbourg et al., 2009; Pagel et al., 2012) using the Laser Doppler Imaging technique (MoorLDI 5061 and Moor Software Version 3.01, from Moor Instruments).

Bone marrow transplantation
For the bone marrow transplantation, 3 x 10^6 bone marrow cells of C57BL/6-Ly5.1 mice were injected into the tail vein of lethally irradiated (twice 600rads) Nox2-/- mice and vice versa. After 6 weeks, when a stable chimerism was guaranteed with flow cytometry analysis of CD45.1 and CD45.2 cell counts, the mice were used for femoral artery ligation and laser Doppler perfusion measurements. Furthermore, Nox2-/- mice received Nox2-/- bone marrow cells and C57BL/6-Ly5.1 mice received C57BL/6-Ly5.1 bone marrow cells, in order to rule out the possible influence of the transplantation on the experiments.

qRT-PCR analyses
Total RNA from collaterals was extracted with Trizol (Life technologies) and DNA digested with DNase I (Promega). 250ng of total RNA was reverse transcribed with the 1st Strand cDNA synthesis kit (Roche), and cDNA was diluted 1:5 in RNase free water. Quantitative PCR was performed with 1µl diluted cDNA using Power Sybr Green master mix (Life technologies) following manufacturer's protocol and as previously described (Pagel et al., 2012) in a StepOnePlus light cycler (Life technologies). Specific amplification was controlled by melt curve analyses and expression level of MCP-1 was related to the expression levels of the 18S rRNA. On each template three independent qRT-PCR reactions were performed. The primer sequences were as follows: Egr-1, forward, 5'-CGAACAACCCTATGAGCACCTG-3', reverse, 5'-CAGAGGAAGACGATGAAGCAGC-3'; 18S rRNA, forward, 5'-GGACAGGATTGACAGATTGATAG–3', 5'-CTCGTTCGTTATCGGAATTAAC–3'.

Isolation of bone marrow mononuclear cells
C57Bl6J (4-6) mice of 8-12 weeks were sacrificed by cervical dislocation: intact femurs and tibias were removed, and bone marrow cells were harvested by repeated flushing with minimal essential medium. Cells were cultured as described previously (Stassen et al., 2003). Characterization of cells was performed by flow cytometry analysis using anti-mouse c-kit antibody (CD117 from Invitrogen).

Endothelial cells
Mouse coronary endothelial cells were purchased from CellBiologics and cultured as described (CellBiologics Inc).

Vascular smooth muscle cells
Mouse vascular SMCs were isolated as described earlier (Kanse et al., 1997) and cultivated in Iscove's modified medium containing 10% (v/v) heat-inactivated fetal calf serum, 10U/ml penicillin, 10g/ml streptomycin, and 2mM L-glutamine.

Cell proliferation assay
Cell proliferation was determined by a colorimetric immunoassay, which based on the uptake of BrdU during DNA synthesis and the quantitative binding of a monoclonal anti-BrdU-antibody (Roche Diagnostics). Cells were cultivated in a 96-well microtiterplate. Subsequently, supernatants derived from mast cells treated for 1h with ionomycin (1µM, Sigma) or solvent were diluted in serum-free medium to a total volume of 100µl/well. After an incubation period of three days BrdU-incorporation was determined.

Isolation of murine neutrophils and platelets
Murine bone marrow cells were harvested from tibias and femurs of PSGL-1-/-, Nox2-/-, or corresponding wild type mice, respectively, and cultured as previously described (Walzog et al., 1999). Prior to experiments, neutrophils were washed and resuspended in Hank's solution supplemented with 0.25% BSA and 0.1% glucose. Platelet rich plasma from citrated whole blood (wild type or P-selectin deficient mice) was obtained by centrifugation at 200g for 5min. Platelets were pelleted (450g, 10min) and resuspended in a buffer containing 138mM NaCl, 2.7mM KCl, 12mM $NaHCO_3$, 0.4mM NaH_2PO_4, 1mM $MgCl_2$, 5mM D-glucose, 5mM Hepes, pH 7.35. Neutrophil and platelet concentrations were measured in a Beckman Coulter (FL/USA) and adjusted to concentrations of $1x10^3$/µl or $2x10^5$/µl, respectively.

Platelet-neutrophil interaction *in vitro*
For flow cytometry or superoxide anion detection neutrophils were incubated with platelets in an 1:200 ratio at 37°C for 10 or 30min, respectively. PNA formation or surface uPA on neutrophils was measured by flow cytometry (FACS Canto II, BD Biosciences) by incubating cells with FITC-labeled rat anti-mouse CD41 antibody (Cat# 11-0411-81, eBioscience), the corresponding rat isotype control IgG1 FITC (Cat# 11-4301-81, eBioscience), anti-uPA rabbit polyclonal antibody (H140, Cat# sc14019, Santa Cruz; labelled with Alexa fluor 488 labeling kit, life technologies), or the rabbit polyclonal isotype control (Cat# CTL-4112, Biolegend), respectively. Co-staining with an APC-labelled anti-Ly-6G antibody (Cat# 17-5931-81, eBioscience) was performed to identify the neutrophil population. To detect superoxide anion release neutrophil suspensions (Hank's solution, 0.25% BSA, 0.1% glucose) were supplemented with 0.5mg/ml cytochrome C (Sigma) prior to incubation with platelets. Supernatants were transferred to a 96-well plate and absorbance was measured at 550nm. To exclude reduction from radicals others than superoxide anions, samples supplemented with 200U/ml superoxide dismutase (SOD; Roche) were measured in parallel and values were subtracted from values without SOD.

Co-culture of mast cells and neutrophils
300 µl of human mast cells (HMC-1) were seeded into a 24 well plate (2 x 10^6 cells/ml) in RPMI medium without FCS. After 2 hours filter inserts with a pore size of 0.4 µm (BD Biosciences) containing either 100 µl of RPMI or 100 µl of freshly isolated human neutrophils (500000 cells) were placed above the mast cells. To activate neutrophils, phorbol 12-myristate 13-acetat (PMA, Sigma-Aldrich) was added to the neutrophils and as a control also to medium-containing filter inserts.
After 3 hours, filter inserts containing medium or neutrophils were removed and supernatants of HMC-1 were used for β-hexosaminidase assay. In brief, supernatants were incubated with 26 mM citrate buffer (pH4.5) and 2.3 mg/ml p-nitrophenyl N-acetyl-α-D-glucosaminide for 90 min at 37 °C. The reaction was stopped by adding 0.4 mM glycine (pH 10.7), and the absorbance was measured at 405 and 570 nm using a multiplate reader.

References
Deindl, E., Ziegelhoeffer, T., Kans, S.M., Fernandez, B., Neubauer, E., Carmeliet, P., Preissner, K., and Schaper, W. (2003). Receptor-independent role of the urokinase-type plasminogen activator during arteriogenesis. FASEB J *10.1096/fj.01-0563fje*.
Drechsler, M., Megens, R.T., van Zandvoort, M., Weber, C., and Soehnlein, O. (2010). Hyperlipidemia-triggered neutrophilia promotes early atherosclerosis. Circulation *122*, 1837-1845.
Dudeck, A., Dudeck, J., Scholten, J., Petzold, A., Surianarayanan, S., Kohler, A., Peschke, K., Vohringer, D., Waskow, C., Krieg, T., *et al.* (2011). Mast cells are key promoters of contact allergy that mediate the adjuvant effects of haptens. Immunity *34*, 973-984.
Goto, S., Ichikawa, N., Lee, M., Goto, M., Sakai, H., Kim, J.J., Yoshida, M., Handa, M., Ikeda, Y., and Handa, S. (2000). Platelet surface P-selectin molecules increased after exposing platelet to a high shear flow. International angiology : a journal of the International Union of Angiology *19*, 147-151.
Juremalm, M., Hjertson, M., Olsson, N., Harvima, I., Nilsson, K., and Nilsson, G. (2000). The chemokine receptor CXCR4 is expressed within the mast cell lineage and its ligand stromal cell-derived factor-1alpha acts as a mast cell chemotaxin. European journal of immunology *30*, 3614-3622.

Kanse, S.M., Benzakour, O., Kanthou, C., Kost, C., Lijnen, H.R., and Preissner, K.T. (1997). Induction of vascular SMC proliferation by urokinase indicates a novel mechanism of action in vasoproliferative disorders. Arterioscler Thromb Vasc Biol *17*, 2848-2854.

McGowen, A.L., Hale, L.P., Shelburne, C.P., Abraham, S.N., and Staats, H.F. (2009). The mast cell activator compound 48/80 is safe and effective when used as an adjuvant for intradermal immunization with Bacillus anthracis protective antigen. Vaccine *27*, 3544-3552.

Plesner, T., Ploug, M., Ellis, V., Ronne, E., Hoyer-Hansen, G., Wittrup, M., Pedersen, T.L., Tscherning, T., Dano, K., and Hansen, N.E. (1994). The receptor for urokinase-type plasminogen activator and urokinase is translocated from two distinct intracellular compartments to the plasma membrane on stimulation of human neutrophils. Blood *83*, 808-815.

Stassen, M., Muller, C., Richter, C., Neudorfl, C., Hultner, L., Bhakdi, S., Walev, I., and Schmitt, E. (2003). The streptococcal exotoxin streptolysin O activates mast cells to produce tumor necrosis factor alpha by p38 mitogen-activated protein kinase- and protein kinase C-dependent pathways. Infect Immun *71*, 6171-6177.

Vincent, L., Vang, D., Nguyen, J., Gupta, M., Luk, K., Ericson, M.E., Simone, D.A., and Gupta, K. (2013). Mast cell activation contributes to sickle cell pathobiology and pain in mice. Blood *122*, 1853-1862.

Walzog, B., Weinmann, P., Jeblonski, F., Scharffetter-Kochanek, K., Bommert, K., and Gaehtgens, P. (1999). A role for beta(2) integrins (CD11/CD18) in the regulation of cytokine gene expression of polymorphonuclear neutrophils during the inflammatory response. FASEB J *13*, 1855-1865.